Available online at www.sciencedirect.com

ScienceDirect

Geochimica et Cosmochimica Acta 131 (2014) 323–343

Geochimica et Cosmochimica Acta

www.elsevier.com/locate/gca

Rainfall and cave water isotopic relationships in two South-France sites

D. Genty [a,*], I. Labuhn [a], G. Hoffmann [a,b,c], P.A. Danis [d], O. Mestre [e], F. Bourges [f], K. Wainer [g], M. Massault [h], S. Van Exter [h,i], E. Régnier [a], Ph. Orengo [a], S. Falourd [a], B. Minster [a]

[a] *Laboratoire des Sciences du Climat et de l'Environnement (LSCE/IPSL), UMR 8212 (CEA/CNRS/UVSQ), Orme des Merisiers, 91191 Gif-sur-Yvette, France*

[b] *Institute for Marine and Atmospheric Research Utrecht (IMAU), Utrecht University, Princetonplein 5, 3584 CC Utrecht, Netherlands*

[c] *Estación Biológica de Doñana CSIC, c/Americo Vespucio, s/n, Isla de la Cartuja, 41092 Sevilla, Spain*

[d] *Pôle d'Etudes et Recherches Hydro-écologie des plans d'eau, IRSTEA, Unité Hydrobiologie HYAX, 3275 route Cézanne, CS 40061, 13182 Aix-en-Provence cedex 5, France*

[e] *Météo-France, Direction de la Climatologie, 42 av. Gaspard-Coriolis, 31057 Toulouse cedex, France*

[f] *Géologie-Environnement-Conseil, 30, rue de la République, 09200 Saint-Girons, France*

[g] *Dept. of Earth Sciences, Oxford University, South Parks Road, Oxford OX13AN, United Kingdom*

[h] *IDES, Université de Paris XI, bât. 504, 91400 Orsay cedex, France*

[i] *UMR HydroSciences Montpellier, Maison des Sciences de l'Eau de Montpellier, UM2, 34095 Montpellier Cedex 5, France*

Received 1 October 2013; accepted in revised form 30 January 2014; Available online 12 February 2014

Abstract

This article presents isotopic measurements ($\delta^{18}O$ and δD) of precipitation and cave drip water from two sites in southern France in order to investigate the link between rainfall and seepage water, and to characterize regional rainfall isotopic variability. These data, which are among the longest series in France, come from two rainfall stations in south-west France (Le Mas 1996–2012, and Villars 1998–2012; typically under Atlantic influence), and from one station in the south-east (Orgnac 2000–2012; under both Mediterranean and Atlantic influence). Rainfall isotopic composition is compared to drip water collected under stalactites from the same sites: Villars Cave (four drip stations 1999–2012) in the south-west, and Chauvet Cave (two drip stations 2000–2012) in the south-east, near Orgnac. The study of these isotopic data sets allows the following conclusions to be drawn about the rainfall/drip water relationships and about rainfall variability: (1) the cave drip water isotopic composition does not show any significant changes since the beginning of measurements; in order to explain its isotopic signature it is necessary to integrate weighted rainfall $\delta^{18}O$ of all months during several years, which demonstrates that, even at shallow depths (10–50 m), cave drip water is a mixture of rain water integrated over relatively long periods, which give an apparent time residence from several months to up to several years. These results have important consequences on the interpretation of proxies like speleothem fluid inclusions and tree-ring cellulose isotopic composition, which are used for paleoclimatic studies; (2) in the Villars Cave, where drip stations at two different depths were studied, lower $\delta^{18}O$ values were observed in the lower galleries, which might be due to winter season overflows during infiltration and/or to older rain water with a different isotopic composition that reaches the lower galleries after years; (3) local precipitation is characterized by local meteoric water lines, LMWL, with $\delta^{18}O/\delta D$ slopes close to 7 in both areas, and correlations between air temperature and precipitation $\delta^{18}O$ are low at both monthly and annual scales, even with temperature weighted by the amount of precipitation; (4) the mesoscale climate model REMOiso, equipped with a water isotope module, allows the direct comparison of modeled and

* Corresponding author. Tel.: +33 1 69082866.
E-mail address: dominique.genty@lsce.ipsl.fr (D. Genty).

http://dx.doi.org/10.1016/j.gca.2014.01.043

observed long term water isotope records. The model slightly overestimates rainfall $\delta^{18}O$ at the respective sampling stations. However, it simulates very well not only the seasonal rainfall isotopic signal but also some intra-seasonal patterns such as a typical double-peak $\delta^{18}O$ pattern in winter time.

1. INTRODUCTION

The isotopic composition ($\delta^{18}O$ and δD) of precipitation is a key parameter used to better understand the present-day atmospheric circulation and, when dealing with fossil waters, of past periods (Sturm et al., 2005). Precipitation $\delta^{18}O$ is often the controlling factor for the isotopic composition of paleo-archives used to reconstruct the climate of the past: for example, precipitation $\delta^{18}O$ controls a large part of the isotopic composition of speleothem calcite (Wang et al., 2001; McDermott, 2004; McDermott et al., 2011), lake ostracod calcite (von Grafenstein et al., 1996), tree-ring cellulose (McCarroll and Loader, 2004; Treydte et al., 2007), soil secondary calcite (Marlin et al., 1993), human teeth (Daux et al., 2005), landsnails (Lecolle, 1983, 1985), beetles (van Hardenbroek et al., 2012), and other archives where the water molecule is involved. Besides, direct records of past precipitation $\delta^{18}O$ can be obtained from ice cores from Greenland, Antarctica and continental glaciers, as well as from fossil waters found in aquifers (Rozanski and Dulinski, 1987) or in fluid inclusions trapped in speleothems (Vonhof et al., 2006), which are composed of fossil precipitation water. The latter can be used to reconstruct past temperatures with the help of speleothem calcite $\delta^{18}O$ and clumped-isotope $\Delta 47$ measurements (Daeron et al., 2011). Consequently, measurements of precipitation $\delta^{18}O$ open the possibility of calculating past continental climate parameters such as temperature, humidity or precipitation $\delta^{18}O$, which are closely linked to air circulation patterns.

Long precipitation $\delta^{18}O$ time series allow the comparison of the isotopic signal with meteorological measurements and the calibration of proxy records (Anderson et al., 2002). Since long local measurement series are not always available, model simulations can be used instead to investigate the link between precipitation and the isotopic proxy. However such an approach needs careful evaluation of the respective proxy forward model. Atmospheric circulation, cloud physics, in particular the role of convective precipitation, and atmosphere-surface interactions have a strong influence on water isotope composition and need to be validated in order to extend the modeled relationships between the water isotopes and various climate parameters to the distant climatic past. A large number of general circulation models are equipped with water isotope modules, allowing the computation of $\delta^{18}O$ and δD patterns of all water reservoirs represented by the respective model (Joussaume et al., 1984; Hoffmann et al., 2000; Schmidt et al., 2007). More recently, high-resolution mesoscale models (potentially with a spatial resolution of ~15 km) were fitted with such isotope modules as well (Sturm et al., 2007; Sjolte et al., 2011). Long time series of $\delta^{18}O$ are of primary importance to verify and test the models' capacity to represent crucial features of the hydrological cycle on seasonal, interannual and decadal time scales.

Although it is well known that cave drip water $\delta^{18}O$ is controlled by precipitation $\delta^{18}O$, the temporal relationship between them is still not well constrained because long monitoring series of both drip waters and local rainfall are rare. The main questions are: which months contribute to the underground recharge that feeds stalactites? What is the average residence time of the mixing reservoir in the soil and bedrock before the water reaches the cave? Several recharge models involving diffuse and fracture flows linked to the great variety of porosity in karst formation hosting the cave have been proposed (Fairchild and Baker, 2012). These models were developed based on (1) geochemical data of drip water (i.e. Mg/Ca; (Tooth and Fairchild, 2003; Fairchild et al., 2006)); (2) fluorescent dye experiments, which are rare because of the complexity of the fracture network (Bottrell and Atkinson, 1992); and (3) the study of water isotopes ($\delta^{18}O$, δD and tritium).

Isotope time series of both rainfall and cave drip water at the same place during several months or years have been investigated in only a few studies. Most of these have revealed that isotope ratios in the cave drip water are very stable compared to the well-marked seasonal changes of the rain water, as in Carlsbad Cavern, New Mexico (Chapman et al., 1992), Waitomo Cave, New-Zealand (Williams and Fowler, 2002), in Bunker Cave, Germany (Kluge et al., 2010), and Nerja cave, Spain (Caballero et al., 1996). In some specific caves, a significant seasonal $\delta^{18}O$ variation is detected in the dripwater because of evaporation processes in the soil and epikarst, like in Soreq Cave, Israel (Bar-Matthews et al., 1996) or mid-western USA caves (Denniston et al., 1999). Strong rainfall events and a rapid connection through the epikarst zone, as is the case with Santana Cave, Brazil (Cruz et al., 2005) or on Socotra Island, Yemen (van Rampelbergh et al., 2013) can also cause seasonal variability. The conclusion of most studies is that cave drip water $\delta^{18}O$ is close to the weighted mean precipitation $\delta^{18}O$ of the year (Yonge et al., 1985; Williams and Fowler, 2002); however, since most time series are short (i.e. from a few months to 2–4 years of monitoring), no modeling has been attempted to closely link rain and cave $\delta^{18}O$ values and to give an average residence time of the water in the karstic zone above the cave.

This article presents the results of stable oxygen and hydrogen isotope monitoring in precipitation at three sites in the south of France: Le Mas, Villars and Orgnac (Fig. 1). Close to these sites, the drip water from several stalactites was monitored in two caves which are known for their prehistoric remains and for their speleothem-based paleoclimatic reconstructions: Villars Cave and Chauvet

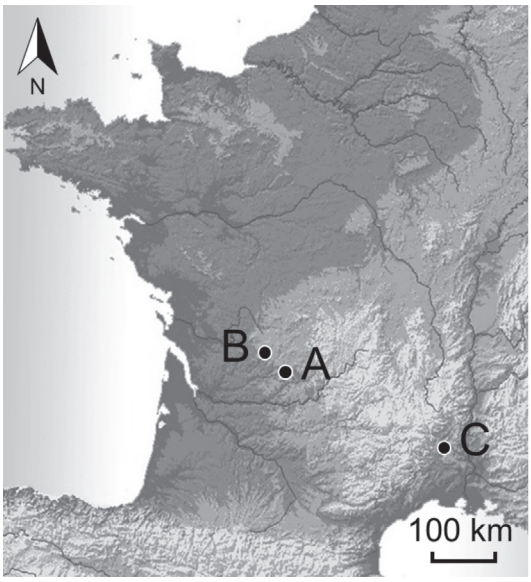

Fig. 1. Locations of the precipitation sampling stations and the corresponding cave sites. (A) Le Mas; (B) Villars/Villars cave; (C) Orgnac/Chauvet cave.

Cave. A better knowledge of the relationship between rainfall $\delta^{18}O$ and drip water $\delta^{18}O$ is of primary importance for the understanding of $\delta^{18}O$ variations found in speleothems and isotope-based climate reconstructions, especially those involving fossil water trapped in speleothem fluid inclusions (Rozanski et al., 1997; Matthews et al., 2000; Vonhof et al., 2008; Zhang et al., 2008; Dublyansky and Spotl, 2009; De Cisneros et al., 2011; Wainer et al., 2011). The age of the drip water feeding stalagmites determines the time representativeness of fluid inclusions and helps in the interpretation of calcite $\delta^{18}O$ records. The data sets presented here from rainfall stations and nearby caves cover more than a decade and provide a unique opportunity to clarify the link between rainfall and cave drip water $\delta^{18}O$.

2. STUDY SITES

The three rainfall monitoring stations have been chosen to be as close as possible to the caves where seepage water monitoring and speleothem studies are conducted (Fig. 1; Table 2). Meteorological data were obtained from the closest meteorological stations which give daily temperature and precipitation data that can be reasonably interpolated to the rainfall stations. In order to simplify the text, the main sites are as follows: Le Mas, Villars and Orgnac, keeping in mind that there are a few kilometres between meteorological, rainfall isotope monitoring and cave stations (Table 2).

The sites of Le Mas and Villars, located about 150 km from the Atlantic ocean in south-west France, are under a typical maritime climate with mild winters (an average temperature of 5.6 °C and 274 mm of precipitation during December, January and February for Villars) and relatively humid summers (an average temperature of 19.3 °C during June, July and August and 212 mm of precipitation for Villars) (Fig. 2a). Note that, despite their proximity, Villars is slightly colder (0.8 °C during June, July and August) than Le Mas because it is closer to the higher plateau of the crystalline terrains of the Limousin (near the Massif Central). Much closer to the Mediterranean Sea, the Orgnac site experiences drier and warmer summers (22.5 °C and 153 mm during June, July and August) (Fig. 2g) and intense precipitation events (e.g. 400 mm on 9–10 September 2002). This site is also characterized by higher precipitation variability (Fig. 2h).

Villars and Chauvet (close to Orgnac) cave sites have already been described in previous studies (Genty et al., 2001, 2006; Genty, 2008). Villars Cave has developed in Bajocian limestone (middle Jurassic), while the Chauvet Cave has developed in hard and compact Barremian limestone (lower Cretaceous). In Villars Cave, drip stations are from small soda-straw stalactites (3–5 cm) that are directly connected to the gallery vault. Microfissures, not visible, likely feed these stalactites but a diffuse flow through the oolithic matrix of the limestone is possible too. In Chauvet Cave, the compact aspect of the limestone likely favor a more direct water flow through the fissures. Both caves are relatively shallow caves: Chauvet is about 50 m from the surface, and Villars is 10–30 m deep. It is important to know the recharge altitude of each cave and to check that it is similar to the altitude of the related meteorological station in order to avoid a bias due to the altitude effect on rainfall stable isotopes, which is generally close to $-0.3‰$/100 m but can be very variable (Clark and Fritz, 1999). On all studied sites the distance and altitude differences between the cave recharge area and the rainfall station are negligible: Villars Cave's recharge area is between 10 and 20 m higher than the rainfall station (175 m a.s.l.); the Orgnac rainfall station is at 305 m a.s.l. while the Chauvet Cave recharge area is between 240 and 250 m a.s.l (Table 3).

3. METHODS

The collected data constitute a unique set of isotope values, which is useful for atmospheric and hydrological studies. The precipitation isotope measurements from Le Mas, starting in 1997, represent the second longest published series in France in terms of the time span covered, and the third most extensive in terms of the number of samples. The other two stations, Villars and Orgnac, are also among the longest in France (15 and 12 years, Table 1). The drip water isotope monitoring in Villars Cave since 1997 is likely the longest in the world. Monitoring continues at all sites.

3.1. Precipitation and cave water sampling

Rainfall water was collected using a similar procedure as recommended by the IAEA for the Global Network of Isotope in Precipitation (GNIP) stations (IAEA, 1997): the water is collected in a funnel at a height of 2 m, which is connected to a 5 l tank with a plastic tube. The tank is buried so that temperature variations are dampened; a film of paraffin oil is used to prevent evaporation. A sample is taken from the tank in a 15 ml brown glass bottle with a conic top specifically designed for stable isotopes. Every time the

Table 1
Overview of French GNIP stations (IAEA/WMO, 2006) with monthly δD and $\delta^{18}O$ measurements, completed with the three new stations presented in this study.

Station name	GNIP Code	Latitude	Longitude	Altitude [m]	Start	End	Number of years	Number of samples $\delta^{18}O$	Number of samples δD
BREST PLOUZANE	711001	48°21′36″	−4°34′ 12″	80	1996	2002	6	79	79
ORLEANS-LA-SOURCE	724901	47°54′0″	1°54′ 0″	109	1996	2005	9	111	111
THONON-LES-BAINS	748501	46°22′20″	6°28′ 15″	385	1963	2002	39	465	124
CESTAS-PIERROTON	753001	44°44′17″	−0°46′ 29″	59	2007	2009	2	33	33
DRAIX	758801	44°8′0″	6° 20′ 0″	851	2004	2009	5	58	58
DAX	760301	43°41′0″	−1°4′ 00″	9	1999	2005	6	67	67
CAMPISTROUS	762101	43°7′12″	0°22′ 48″	600	1997	1998	1	15	15
MONTPELLIER	764301	43°34′12″	3°57′ 00″	45	1997	1998	1	20	20
AVIGNON	764501	43°57′00″	4°49′ 12″	30	1997	2009	12	130	129
CARPENTRAS	764601	44°57′00″	5°46′ 48″	99	1997	1998	1	23	23
GARDANNE	765301	43°27′00″	5°27′ 00″	215	1997	1998	1	19	19
MALAUSSENE	768801	43°55′12″	7°7′ 48″	359	1997	1998	1	13	13
PONTE LECCIA	778701	42°28′48″	9°12′ 0″	200	1997	1998	1	12	12
Le Mas	–	45°7′45″	1°11′31 E	191	1997	2012	16	111	109
Villars-Doggy	–	45°26′18″	0°47′2 E	175	1998	2012	15	86	83
Orgnac	–	44°19′8″	4°24′47 E	305	2000	2012	12	84	83

water is collected, the amount of water in the container is measured. Thus, for each isotope value the corresponding amount of precipitation for the water collection period is known. Some of these values of precipitation amount are missing. In order to fill the gaps of missing measurements and to check the amount of water measured in the container, sums are calculated for each sampling period from daily precipitation data from the corresponding meteorological stations. Despite the sometimes irregular sampling interval (see Table 4 for the sampling dates), samples are taken continuously, so that each sample consists of all precipitation since the preceding sampling date, and the whole year's precipitation is collected. This is important because it allows the calculation of weighted seasonal or annual averages. Drip water in Villars Cave was sampled on the same dates as precipitation. The sampling interval in Chauvet was larger due to limited access to the cave (see Table 7 for the number of samples and Figs. 10 and 11 for sampling dates in each cave). The water was collected in a 15 ml brown glass bottle at the tip of each stalactite. The time to fill the bottles varies from few minutes to few hours depending on the sampling station and the season. As no significant variability in the drip water isotopic composition is observed here, "instantaneous" samples are representative of the seepage water composition between each sampling. Moreover, it is not necessary to weight the drip water $\delta^{18}O$ by the drip rate as we do for the rainwater; we did the calculation for the most variable drip station (Villars #10A), and the weighted $\delta^{18}O$ is in the error margin of the unweight one (see Table 7).

3.2. Calculation of monthly $\delta^{18}O$ values to create a time series with regular time steps

It was not possible to take precipitation samples on a monthly basis. Although the monthly time step for sampling precipitation is arbitrary (i.e. it has no hydrological basis), our irregular sampling interval makes it difficult to compare the measurements directly to monthly meteorological data and to calculate mean values over different months. Therefore, a new time series of monthly rainfall $\delta^{18}O$ values was created based on the $\delta^{18}O$ measurements and on daily precipitation data from the closest meteorological stations. The $\delta^{18}O$ value of a given sampling period is assigned to each day of this period. Then the monthly isotopic composition $\delta^{18}O_m$ is calculated as the mean $\delta^{18}O$ of all days of the calendar month, weighted by the amount of precipitation:

$$\delta^{18}O_m = \frac{\sum_{i=1}^{n} P_i * \delta^{18}O_i}{\sum_{i=1}^{n} P_i}$$

where P_i is the daily precipitation amount, $\delta^{18}O_i$ is the "daily" $\delta^{18}O$ value, 1 is the first and n the last day of the respective month m. $\delta^{18}O_m$ is only calculated for those months where at least 70% of the monthly precipitation is available, which excludes some points near the periods where the sampling was interrupted. The time series of recalculated monthly $\delta^{18}O$ and δD values are very similar to the original time series for all three stations (see example in Fig. 3).

3.3. Measurements

Hydrogen isotopes (δD) were measured on an ISOPRIME mass spectrometer and a PICARRO laser spectrometer. The 1 sigma error for both methods is ±0.5‰. Oxygen isotopes ($\delta^{18}O$) were measured on a Finnigan MAT 252 by equilibration with CO_2. The 1 sigma error of the $\delta^{18}O$ is ±0.05‰. Early measurements in 1997 and 1998 were performed on a VG SIRA IRMS with an error of ±0.2‰ for the $\delta^{18}O$ while δD was measured using the zinc reduction method with an error close to ±2‰.

3.4. The mesoscale model REMOiso

The REMO (REgional MOdel) model was derived from the European weather forecast model of the Deutscher Wetterdienst (Jacob and Podzun, 1997) and then updated

Table 2
The three studied sites as referred to in the text. The rainfall isotope stations are given with the respective meteorological stations and caves and their corresponding distances from the isotope stations (in km).

Site	Rainfall isotope station	Meteorological station	Cave
Le Mas	Le Mas	Montignac/Brive (7.9/27)	Villars (50)
Villars	Villars-Doggy	Nontron (13.5)	Villars (0.4)
Orgnac	Orgnac (Museum)	Orgnac (Bruguier) (3.0)	Chauvet (7.3)

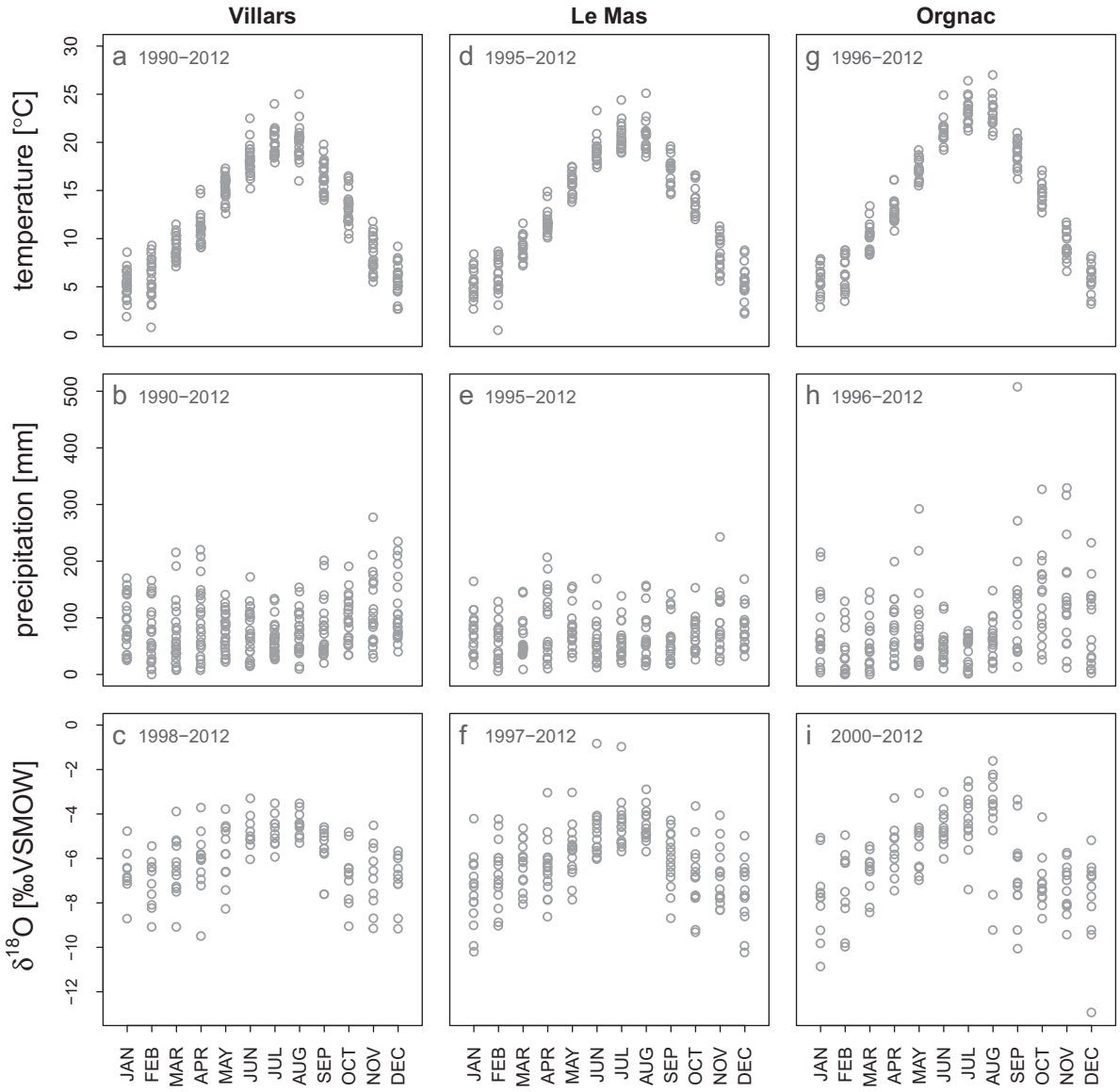

Fig. 2. Variability of mean monthly temperature, monthly precipitation sums and monthly precipitation $\delta^{18}O$ at the studied sites: Villars, Le Mas and Orgnac.

with ECHAM-4 physics (Jacob, 2001). The model solves the full equations of conservation of mass, energy and momentum on a numerical grid ("primitive equations"). The principal prognostic variables are T (temperature), q (specific humidity), $\mathbf{v}$ (three dimensional wind vector). Most physical processes (e.g. cloud formation, soil hydrology, etc.) are solved on a sub-grid scale and are parameterised, that means that the effect of these sub-grid processes on the resolved scale is computed using often empirical relationships between the respective variables and large scale variable (for example the relation between the concentration of aerosols and cloud coverage). In a following step REMO was equipped with a module allowing the computation of the water isotopes in all compartments of the

Table 3
Coordinates, geology, vegetation and external meteorological characteristics of the studied caves.

Cave	Cave latitude, longitude, altitude and (average depth)	Precipitation [mm/year]	Annual temperature [°C] (DJF/JJA)	Geology	Vegetation
Villars	45°26′N, 0°47′E, 175 m (12–25 m)	1005 mm	12.4 (5.6/19.3)	Oolithic limestone Bajocian (Jurassic)	Temperate vegetation, Oaks, hornbeams
Chauvet	44°23′N, 4°24′E, 205 m (40–60 m)	977 mm	14.1 (6.1/22.5)	Compact limestone Baremian (Cretaceaous)	Mediterranean vegetation (bushes, green oaks)

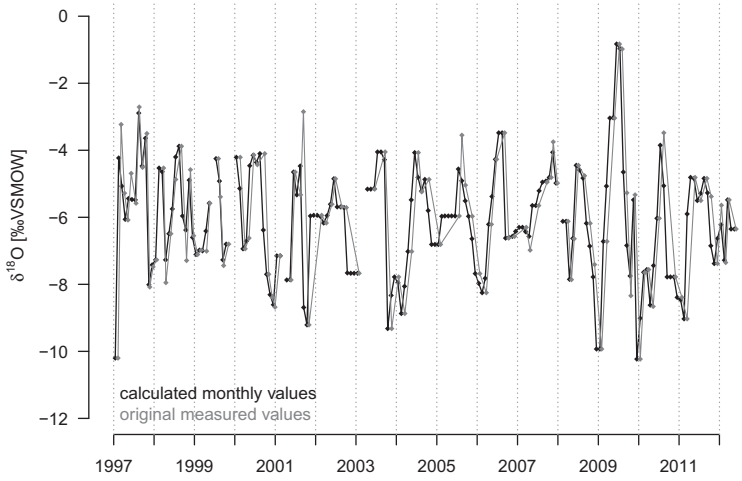

Fig. 3. Comparison between calculated monthly $\delta^{18}O$ values (in black) and the original measured values (in grey) using the example of Le Mas. The slight shift between the two curves appears because the date assigned to each monthly value is the 15th of that month, whereas the date for the original values is the last day of the sampling period.

model's hydrological cycle. The respective model version is called REMOiso and discussed in (Sturm et al., 2005, 2007). The standard spatial resolution of REMOiso, which was also used in this study is 0.5°*0.5°, with 19 vertical layers and a time step of 5 min. The mesoscale model covers typically an area of several thousand square kilometres and obviously needs information on all relevant three-dimensional climate parameters at the borders of its numerical grid. It is therefore embedded in a global circulation model which is equally equipped with a water isotope module (ECHAM4iso) (Hoffmann et al., 1998). Further details about the embedding technique are described in detail in (von Storch et al., 2000). It involves in particular the spectral nudging of the mesoscale model's wind fields towards the global model's winds. The ECHAM4 winds are also nudged toward ECMWF re-analysis winds (ERA40, (Uppala et al., 2005)). This double nudging technique (ERA40 → ECHAM4iso → REMOiso) is aimed at allowing a dynamically coherent high-resolution simulation close to the real observed synoptic variability. In summary, the REMO model needs the information of the state of the atmosphere (T, q, $\mathbf{v}$) at its boundaries and additionally in its nudged mode the observed wind field within its numerical domain. The entire simulated time period covers the time period from 1958 to 2001. Here, we focus only on the period of overlap between model and our in situ measurements in the 1990s and early 2000s.

4. RESULTS AND DISCUSSION

The first part of the results describes the rainfall isotopic time series, which are compared to the other available series and characterized by their meteoric water lines. We discuss the temperature/$\delta^{18}O$ correlations and the representativeness of REMOiso $\delta^{18}O$ simulations, both being important for the calibration of the speleothem $\delta^{18}O$. In a second part, we present the drip water isotopic time series and then discuss the estimation of the time residence of the infiltrated water in the studied sites using the rainfall data.

4.1. Rainfall isotopic composition characterization

4.1.1. Results

Seasonal variations, local meteoric water lines and comparison with other French GNIP records. The three rainfall isotopic stations Villars, Le Mas and Orgnac display similar seasonal isotopic variations compared to other French GNIP stations (Fig. 4, Supplementary material Table 4). Note the particularly similar behavior between the Orgnac station and Avignon and Draix, with, for example, low $\delta^{18}O$ values during winter 2006/07 and 2008/09 or high values during summer 2006. The seasonal amplitude is larger at most of these stations between 2004 and 2010; this is noticeable during the year 2008/2009 where Le Mas and Orgnac stations registered about a 9‰ amplitude change

between winter 2008/09 and summer 2009. Large changes also occurred between 2005 and 2006. After 2010, the seasonal amplitude is reduced again (Fig. 4).

Fig. 2 shows annual cycle graphs of monthly $\delta^{18}O$ and δD variations for Le Mas, Villars and Orgnac, where all measured values are plotted. This type of representation is very useful for characterizing the local rainfall isotopic composition, displaying both the monthly isotopic variation (i.e. difference between different months) and the inter-annual variability for a single month. The $\delta^{18}O$ variability is much more pronounced during the winter months than during the summer months, especially for Le Mas (without the exceptional values for the summer of 2009) and Villars, the two Atlantic stations. This is in agreement with larger winter variability of most climate parameters in mid- and high latitudes. At Orgnac, the summer variability is as pronounced as that in winter (Fig. 2i). For all stations, there is an increasing $\delta^{18}O$ trend from winter months (December/January) until August. Then, there is a threshold after which the rainfall isotopic composition decreases more or less abruptly until November/December (Fig. 2c, f and i). Note that this decrease is much more marked at the Orgnac station, likely due to changes in the precipitation regime and the influence of Mediterranean storm tracks, which start to be more frequent at this period (Celle-Jeanton et al., 2004). Average seasonal differences between July–August and January–February are −3.1‰ at Le Mas, −2.1‰ at Villars and −3.6‰ at Orgnac.

Most of the isotopic values from the three stations lie on the global meteoric water line (GMWL), but all the slopes are lower than the global average slope of 8 (Fig. 5). Le Mas and Villars local meteoric water lines (LMWL) are parallel with a similar slope of 7.3 when removing the two points of summer 2009, which show abnormally high values (Fig. 5, Table 4). If these two points are integrated, then the Le Mas LMWL slope would be slightly lower (6.9). It should be noted that such high monthly $\delta^{18}O$ values are often visible on GNIP data sets and are likely due to evaporation during the rainfall in a dry air column (see Figs. 2–18 in (Clark and Fritz, 1999)). Orgnac rainfall data show larger variations and the slope is slightly lower (7.0), but overall the data set is very similar to the two other stations, which are mainly controlled by the Atlantic climate regime.

4.1.2. Discussion

4.1.2.1. Correlations between temperature and rainfall $\delta^{18}O$.

In the middle- and high latitudes, $\delta^{18}O$ is strongly affected by temperature through its control on the rainout of air masses ($\delta^{18}O$ depletion due to evacuation of a condensed phase – the rain – from the cloud vapor (Clark and Fritz, 1999)). The temperature influence on the rainout process is the basis for using the water isotopes in paleoclimate archives like speleothems, tree rings or ostracods for temperature reconstructions. Consequently, it is of first importance to constrain the causes of $\delta^{18}O$ variation at a specific location by studying correlations with temperature. However, while the correlation between rainfall isotopic composition and surface temperature on a global scale is certain (Clark and Fritz, 1999), it is less obvious to quantify it at a specific site because in-cloud temperatures rather than surface temperatures control condensation and

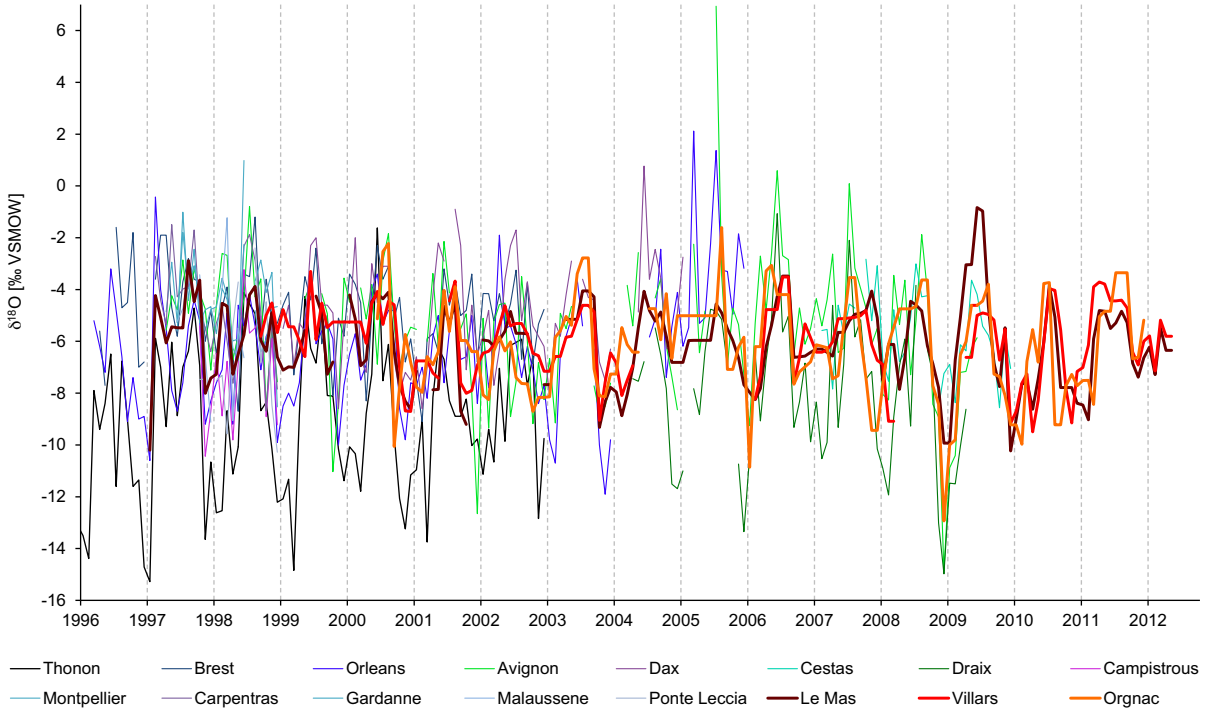

Fig. 4. Monthly precipitation $\delta^{18}O$ time series for all French GNIP stations (IAEA/WMO, 2006) and the new stations presented in this study, Le Mas, Villars and Orgnac.

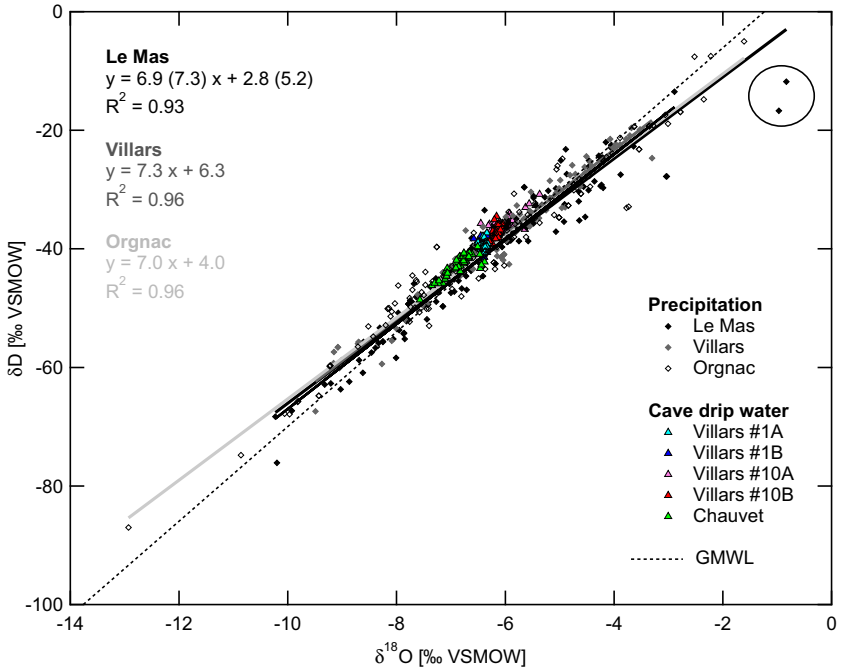

Fig. 5. Scatter plot of δD vs. $\delta^{18}O$ in cave drip water and precipitation, and local meteoric water lines for Le Mas, Villars and Orgnac. For Le Mas, one line is plotted for all the data (slope 6.9) and another line (slope 7.3) without the two data points of summer 2009 (encircled points in the upper right corner). See text for explanation of these outliers. The dotted line is the global meteoric water line (GMWL).

Table 5
Correlations between temperature and precipitation $\delta^{18}O$ on the monthly, seasonal and annual time scale. MMT is the mean monthly temperature, MMPT is the mean monthly temperature weighted by the amount of precipitation.

Site	Monthly		Summer (JJA)	Winter (DJF)	Annual
	$\Delta\delta^{18}O/\Delta MMT$ (R^2)	$\Delta\delta^{18}O/\Delta MMPT$ (R^2)	$\Delta\delta^{18}O/\Delta T$ (R^2)	$\Delta\delta^{18}O/\Delta T$ (R^2)	$\Delta\delta^{18}O/\Delta T$ (R^2)
Le Mas	0.16 (0.35**)	0.18 (0.37**)	0.24 (0.12)	0.51 (0.14)	0.47 (0.14)
Villars	0.14 (0.33**)	0.16 (0.35**)	0.17 (0.10)	−0.11 (0.02)	0.56 (0.35)
Orgnac	0.18 (0.37**)	0.18 (0.37**)	0.33 (0.10)	0.95 (0.42*)	0.05 (0.00)

The first number is the slope of the linear regression line in ‰/°C, the number in parentheses is the linear correlation coefficient R^2.
* Significance level: $p < 0.01$.
** Significance level: $p < 0.001$.

Table 6
Weighted mean annual precipitation $\delta^{18}O$ and mean annual temperature for Le Mas, Villars and Orgnac stations.

Year	Le Mas		Villars		Orgnac	
	Weighted mean annual $\delta^{18}O$ [‰]	Mean annual temperature [°C]	Weighted mean annual $\delta^{18}O$ [‰]	Mean annual temperature [°C]	Weighted mean annual $\delta^{18}O$ [‰]	Mean annual temperature [°C]
1997	−5.59	13.3		13.0		14.5
1998	−6.22	12.4		12.1		13.8
1999	−6.33	12.8	−5.40	12.5		14.1
2000	−6.32	13.0	−6.42	12.9		14.3
2001	−7.69	12.6	−6.62	12.3	−6.15	14.1
2002	−6.62	13.0	−5.90	12.8	−7.63	14.4
2003	−6.72	13.5	−6.50	13.5	−6.55	14.6
2004	−6.43	12.3		12.2	−5.45	13.7
2005	−6.17	12.4		12.4	−6.30	13.5
2006	−6.44	13.3	−6.13	13.2	−6.04	14.3
2007	−5.66	12.8	−5.78	12.5	−6.96	14.3
2008	−6.82	12.4		11.9	−6.60	13.6
2009	−5.31	12.9	−6.53	12.5	−7.64	14.5
2010	−7.36	11.8	−7.49	11.3	−7.71	13.2
2011	−6.20	13.6	−5.48	13.6	−6.05	15.0

isotope fractionation. Surface temperature from meteorological stations is often the only available data, but it disregards all the processes that occur outside the clouds, like air mass mixing or evaporation. Furthermore, it is preferable to consider the temperature when it rains and not the averaged air temperature. As done by (Kohn and Welker, 2005), we investigated the correlations between mean monthly temperature (MMT) and rainfall $\delta^{18}O$, and between the mean monthly temperature weighted by the daily amount of precipitation (MMPT) and rainfall $\delta^{18}O$ (Tables 5 and 6). Results show that MMT and MMPT are generally very similar for the three stations (Fig. 6), with the following small differences:

– for Le Mas and Villars stations, the MMPT is slightly higher than the MMT (+0.6 and +0.2 °C on average respectively) (Fig. 6a and b);

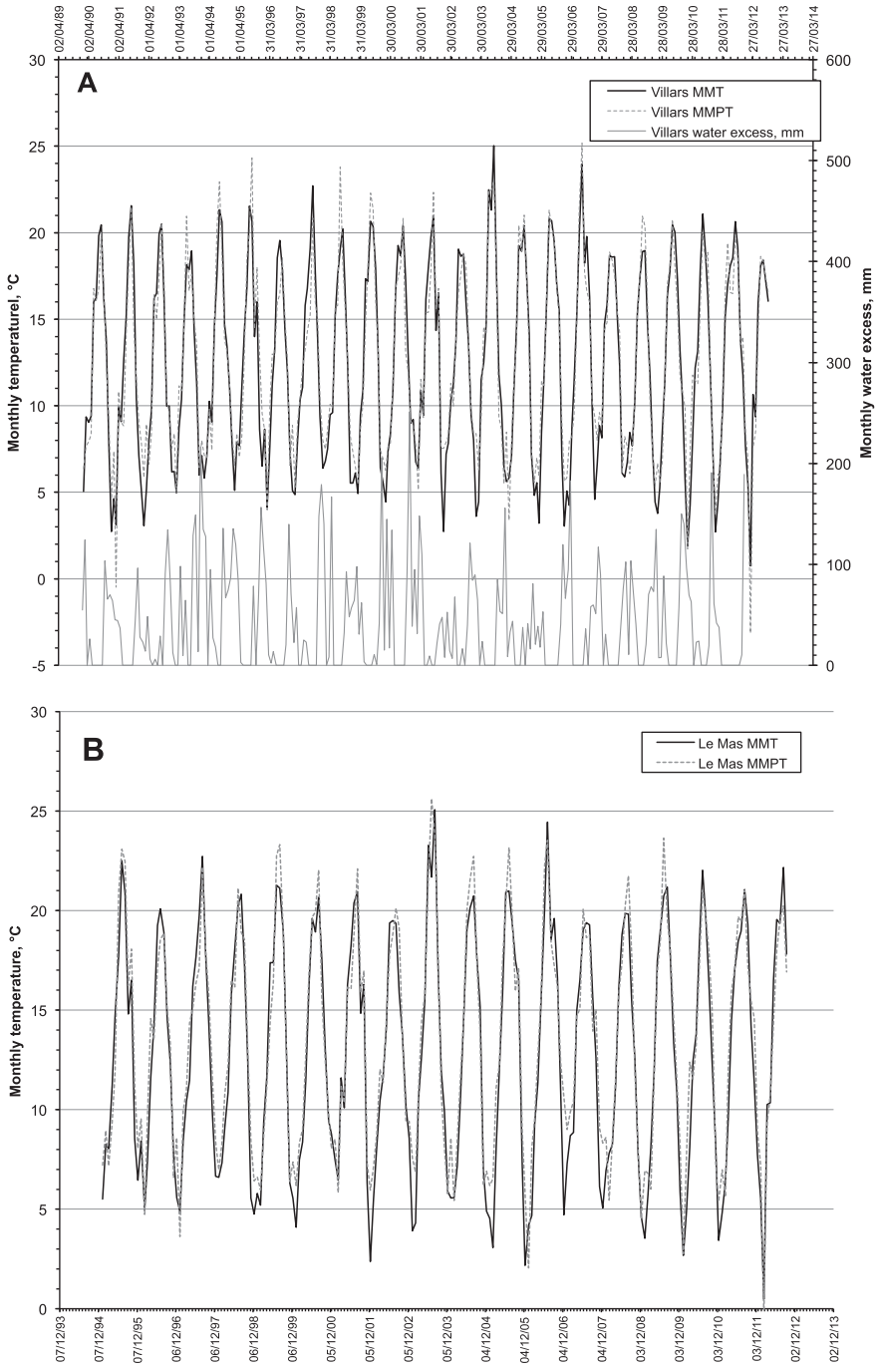

Fig. 6. Comparison of mean monthly temperature (MMT, solid line) and the mean monthly temperature weighted by the amount of precipitation (MMPT, dashed line). The grey curves represent the water excess estimated according to the Thornthwaite formula.

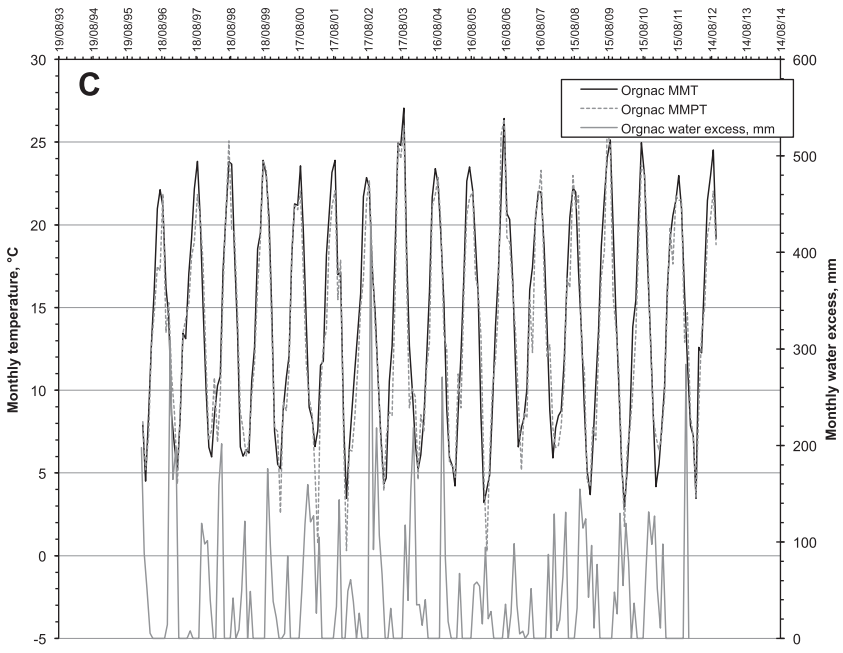

Fig 6. *(continued)*

– for Orgnac, the MMPT is generally lower than the MMT (−0.6 °C on average);. this occurs more often during the winter months (Fig. 6c).

The differences between stations are possibly due to the difference in the precipitation regimes, such as the more pronounced seasonality in the precipitation for the Orgnac station, which is influenced in winter by Mediterranean storms as shown, for example, in data from the nearby station of Avignon (Celle-Jeanton et al., 2001).

Whether MMT or MMPT is considered, the correlations between rainfall $\delta^{18}O$ and mean monthly temperature generally have a low significance (R^2 of 0.33–0.37; Table 5, Fig. 7). The mean values for each month (triangles in Fig. 7) plot close to the linear regression line of all measured monthly values. This suggests that the correlation on a monthly time scale is due to the similar seasonal cycle in both temperature and $\delta^{18}O$ (cf. Fig. 2). We also tested the correlation for winter and summer months separately and found even lower R^2 suggesting no significant correlation. The average slopes between monthly rainfall $\delta^{18}O$ and monthly temperatures (MMT or MMPT) are low and very similar between the stations (0.14–0.18‰/°C; Table 5). Compared with other published data, like those found in North America (0.55‰/°C) (Kohn and Welker, 2005), these values are low. But it is now well known that the T–$\delta^{18}O$ relationship is often linked to site specific circulation patterns and that highly significant correlations are rather rare. Since the global study of Dansgaard (1964), which gave an annual $\Delta\delta^{18}O/\Delta T$ of 0.69, marine and continental data sets have given different slopes, highlighting the importance of local geography (continentality, altitude, latitude etc.). Between continental, marine and polar sites, the annual $\Delta\delta^{18}O/\Delta T$ varies from 0.17 to 0.9‰/°C (Clark and Fritz, 1999).

T–$\delta^{18}O$ dependency has been extensively studied in the past and a general slope for mid-latitude continental stations has yielded a mean slope of 0.58‰/°C (Rozanski et al., 1993). However, it appears that, depending on the location, the slope is highly variable, i.e. from 0.18 to 0.49 in Canada (see examples and references in (Clark and Fritz, 1999)), and, moreover, T–$\delta^{18}O$ correlations are generally weak (Hoffmann et al., 2005) but not always published except rare local studies like the ones near Avignon, relatively close to the Orgnac site (Celle et al., 2000).

Our data lead to similar conclusions: the highest correlation between mean annual temperature (MAT) and mean annual rainfall $\delta^{18}O$ occurs at Villars station ($R^2 = 0.35$), then Le Mas station displays a weak correlation ($R^2 = 0.14$), while Orgnac data are not correlated at all (Fig. 8a). For the two south-western stations, Villars and Le Mas, the T–$\delta^{18}O$ slopes are close to the global one: 0.54‰/°C for Villars and 0.47‰/°C for Le Mas, even if for this last station the low R^2 makes this value uncertain (Fig. 8). As for the mean monthly temperature, correlations with precipitation $\delta^{18}O$ were investigated for the mean annual temperature weighted by the amount of precipitation (MAPT, Fig. 8b). Results are very close to the one obtained using the MAT: a slope of 0.57‰/°C for Le Mas and 0.50‰/°C for Villars. Correlation coefficients are also similar: $R^2 = 0.35$ for Le Mas and slightly higher for Villars ($R^2 = 0.19$), but there no significant correlation for the Orgnac site.

Summarizing the T–$\delta^{18}O$ relationships, whether monthly or annual values, weighted or unweighted temperatures are considered, the correlations between rainfall $\delta^{18}O$ and air surface temperature are very low. Similar results were found in southern France stations, where different air masses from the Atlantic and the Mediterranean

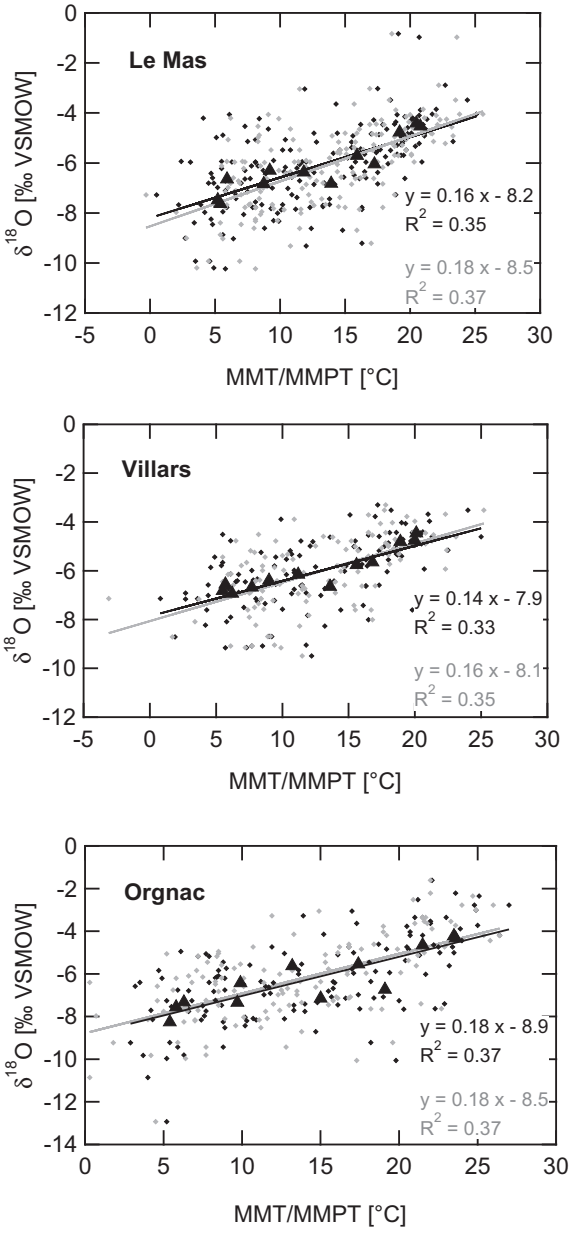

Fig. 7. Scatter plots between mean monthly temperature (MMT, black points) or mean monthly temperature weighted by the amount of precipitation (MMPT, grey points) and monthly precipitation $\delta^{18}O$ for Le Mas, Villars and Orgnac. The triangles represent the mean values for each month (January to December).

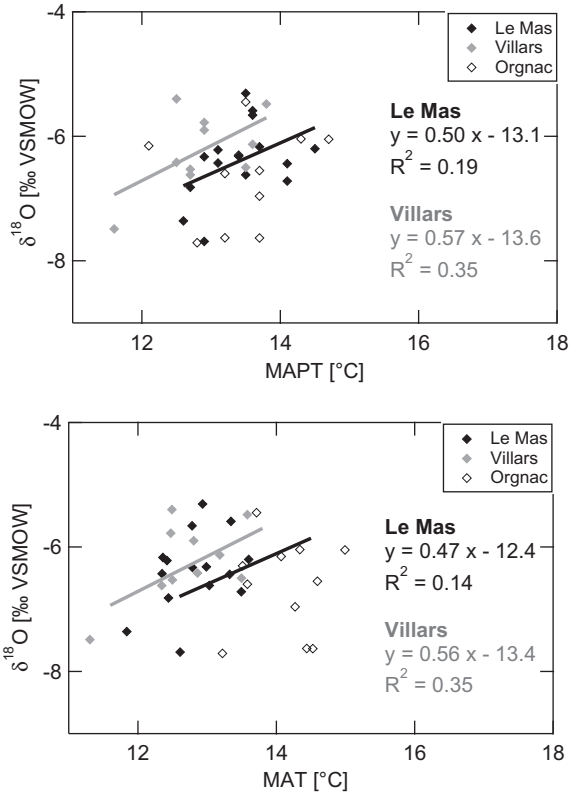

Fig. 8. Scatter plots between mean annual temperature (MAT, top) or mean annual temperature weighted by the amount of precipitation (MAPT, bottom) and mean annual precipitation $\delta^{18}O$ for Le Mas, Villars and Orgnac. The equation of the regression line and R^2 for Orgnac are not given because there is no correlation between annual temperature and precipitation $\delta^{18}O$.

interact. As a consequence, any estimated transfer function between a paleoclimate proxy based on rainfall $\delta^{18}O$ and surface air temperature, is not statistically robust.

4.1.2.2. Comparison of data with REMOiso simulations. REMOiso results were extracted for the respective grid boxes containing the south-west stations Le Mas and Villars, and the Orgnac station in the south-east (Supplementary material Table 9). For technical reasons, the simulation ended in 2001, which is why the period of overlap between the model results and the isotope observations is rather short: 58 months for Le Mas, 39 months for Villars and 18 months for Orgnac (Fig. 9). A comparison between the REMOiso simulation and the rainfall $\delta^{18}O$ measurements shows the following:

- at all sites, the phasing of the seasonal cycle is well simulated;
- for Le Mas and Villars, REMOiso $\delta^{18}O$ is significantly more enriched than measurements, by 1–2‰ during the summer months; winter values are quite well simulated;
- the Orgnac station displays a better agreement between modeled and measured values, but summer months are still slightly overestimated by REMOiso;
- an intriguing result of the REMOiso simulation is the good agreement with parts of the observed intra-annual variability, in particular the double peaks in $\delta^{18}O$, which are clearly observed at Le Mas in February–March and July–August, or the secondary winter peak in December at Orgnac.

For the last point, it is interesting to note that the double peak simulations are not linked to any corresponding temperature or rainfall variations because these two parameters do not show such a pattern. It needs additional analysis to

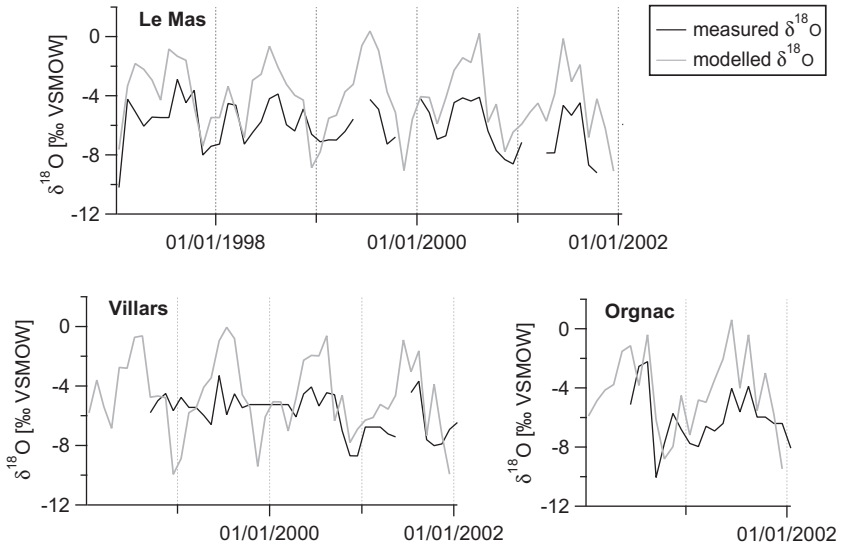

Fig. 9. Comparison between measured precipitation $\delta^{18}O$ (black lines) and REMOiso simulations (grey lines) for Le Mas, Villars, and Orgnac.

(a) confirm the robustness of these peaks in the observation and (b) to investigate the respective causes. Here we only speculate that varying transport lengths and accompanying rainout histories both possibly associated to atmospheric circulation anomalies might have a negligible impact on local temperatures and precipitations but produce a significant change of the isotopic composition of the respective water vapor. It is in any case remarkable that REMOiso is able to reproduce this type of intra-annual variability.

In summary, the double-nudged REMOiso simulation provides a good representation of local rainfall $\delta^{18}O$, although its average level and its seasonal amplitude differ significantly from the observations. The overestimation of the seasonal amplitude, in particular during summer time, points to possible model problems with the representation of convective rain events and their isotopic signatures. It is well known that summer convection is a major challenge for weather forecast models. In particular the exact location, intensity and duration of these events are badly described by GCMs/RCMs in general and insufficiently constraint by the regional wind fields as it was done here in our double nudging approach.

4.2. Comparison between rainfall $\delta^{18}O$ and drip water $\delta^{18}O$ at Villars and Chauvet Cave – importance for cave water residence time and age estimation

Water movement in a karstic structure is guided by three types of porosity: inter-granular pore space, joints and fractures, and larger conduits (Ford and Williams, 2007). Speleothems are mainly fed by joints and fractures and/or millimetric pore spaces (Fairchild and Baker, 2012). Depending on the porosity type of the rock formation above the speleothem, flow time between the surface and the stalactite exit can be highly variable: diffuse flow through micro-fractures or small pores will show dampened seasonal variations while preferential flow through large fractures or conduits will be more sensitive to rainfall events and seasons (Genty, 2008; Fairchild and Baker, 2012). It is of primary importance for speleothem (and dendro-isotopic) paleoclimate studies to know the origin and the average age of the feeding water, especially in a context where paleoclimatic studies focus on annual signals and temperature quantification, both of which require calcite and water $\delta^{18}O$ values (Treble et al., 2005; Daeron et al., 2008; Vonhof et al., 2008). The residence time of cave drip water can be estimated by studying the discharge under stalactites, leading to conceptual models of cave drip water hydrology, but there are few studies dealing with this topic (Friederich and Smart, 1981; Fairchild et al., 2006; Bradley et al., 2010; Wackerbarth et al., 2012). However, even if until now the average age of the seepage water feeding stalagmites in most caves is not well constrained, the following observations have been made: (1) most stalactite drip waters display seasonal variability, with increasing flow rate in late November/early December for middle latitudes of temperate areas (Genty and Deflandre, 1998); (2) the mean residence time of these dripping ground waters is very variable from one site to the other and ranges from a few weeks to one or several years up to decades, as demonstrated by tritium and $\delta^{18}O$ tracers (Yonge et al., 1985; Chapman et al., 1992; Kaufman et al., 2003; Kluge et al., 2010; Oster et al., 2012). This large discrepancy is certainly due to the heterogeneity of the karstic terrains but also to the methods that were used that limit the time delay to seasonality like it was done in some south France sites (e.g. (Bakalowicz and Jusserand, 1986)).

Recently, a model study focused on the mechanistic understanding of the relationship between rainfall $\delta^{18}O$, cave drip water $\delta^{18}O$ and speleothem calcite $\delta^{18}O$ (Wackerbarth et al., 2012). Nevertheless this relationship has never been empirically quantified before using such a long time series, despite its importance for the interpretation of paleoclimatic proxies. Stable isotopes recovered

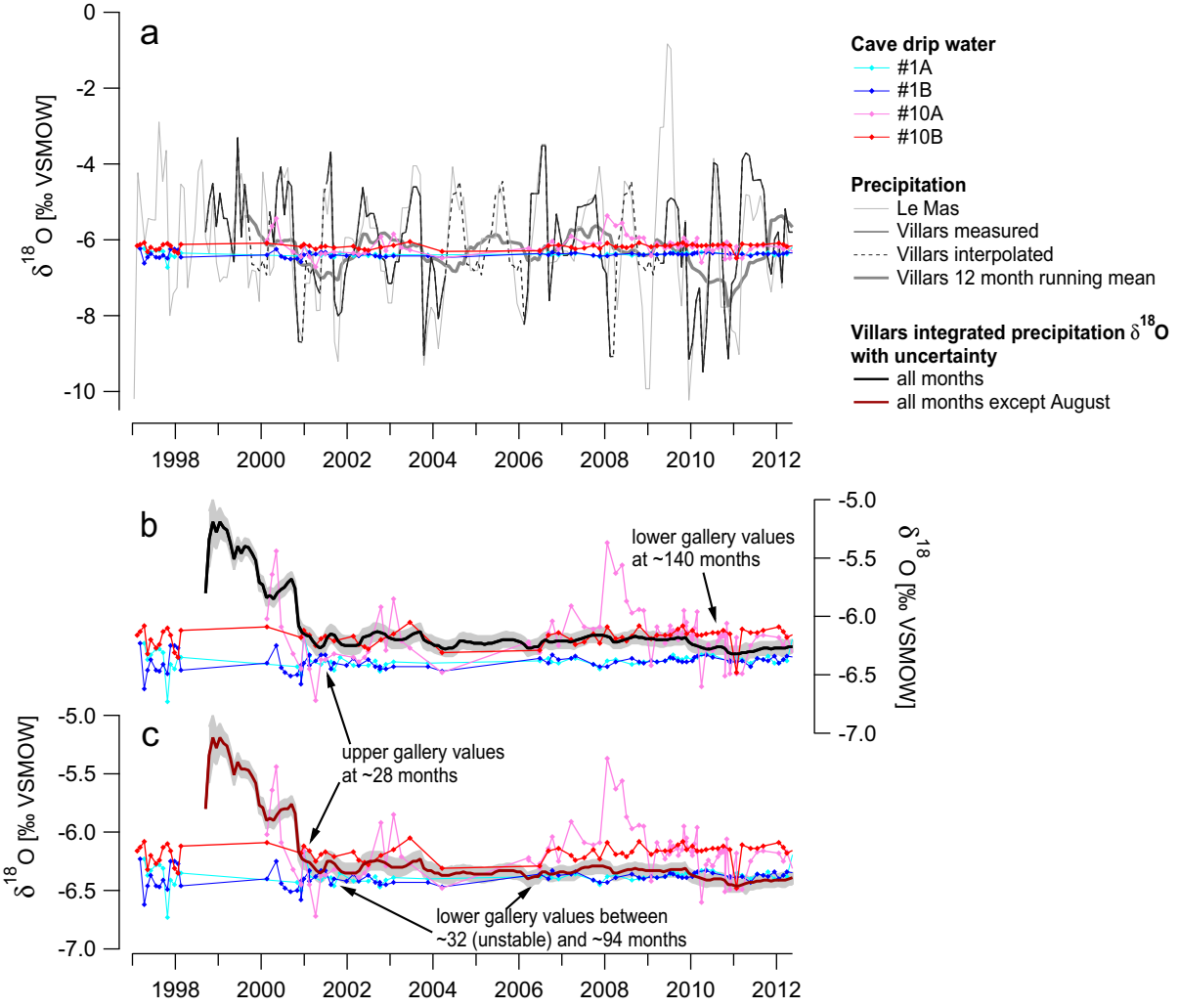

Fig. 10. (a) Precipitation and drip water $\delta^{18}O$ at Villars cave. Light blue and dark blue lines are drip water measurements from the lower gallery (#1A, #1B); pink and red lines are drip water measurements from the upper gallery (#10A, #10B). Grey and black lines are the precipitation $\delta^{18}O$ (black: measured data; black dotted: interpolated data with mean monthly values – see methods section; grey: Le Mas data). The thick grey line is a 12 month running mean of precipitation $\delta^{18}O$ weighted by the amount of precipitation (it considers all months of the year). (b) Drip water $\delta^{18}O$ compared with the integrated precipitation $\delta^{18}O$ for all months (black). (c) Drip water $\delta^{18}O$ compared with the integrated precipitation $\delta^{18}O$ for all months except August (brown). Errors on measurements (±0.05‰ for $\delta^{18}O$, ±0.5 mm for precipitation amount) were added to the variance of the cumulative weighted $\delta^{18}O$ mean, resulting in the upper and lower uncertainties close to ±0.06‰ (grey shading). (For interpretation of the references to colour in this figure legend, the reader is referred to the web version of this article.)

from speleothem fluid inclusions or tree-ring cellulose, for example, both depend on soil water $\delta^{18}O$ rather than rainfall $\delta^{18}O$, which can differ from precipitation due to evaporation, soil water residence time and mixing (see also Wackerbarth et al., 2012). The comparison of rainfall and cave drip water $\delta^{18}O$ on the long time series of Villars/Le Mas and Chauvet/Orgnac allows the construction of a water mixing model to estimate the origin and the age of the infiltration water at these sites.

4.2.1. Results – Cave drip water $\delta^{18}O$ and δD time series

Monitoring of drip water in Villars and Chauvet Cave shows that the stable isotope composition has been very constant since the beginning of measurements (Figs. 10 and 11, Table 7 and Supplementary material Table 8). The four drip stations of Villars represent two depths inside the cave: #10A and #10B are situated in the upper galleries, about 10 m below the surface, while stations #1A and #1B are situated in the lower galleries at about 25 m depth (Genty, 2008). For each gallery level, the $\delta^{18}O$ (like the δD) displays homogeneous values: −6.17‰ ($1\sigma = 0.22$; $N = 86$)) and −6.17‰ ($1\sigma = 0.07$; $N = 67$) for the upper gallery and −6.38‰ ($1\sigma = 0.06$; $N = 70$) and −6.39‰ ($1\sigma = 0.05$; $N = 79$) for the lower gallery (Table 7). In the calculation of mean values, early data measured on the VG mass spectrometer were discarded because of their low accuracy (see Section 3.3; Table 7). Beside the stability of the drip water isotopic signal found in Villars and Chauvet Cave, there is a significant difference of 0.21‰ between the lower and the upper galleries in Villars Cave, the lower gallery having the lowest values

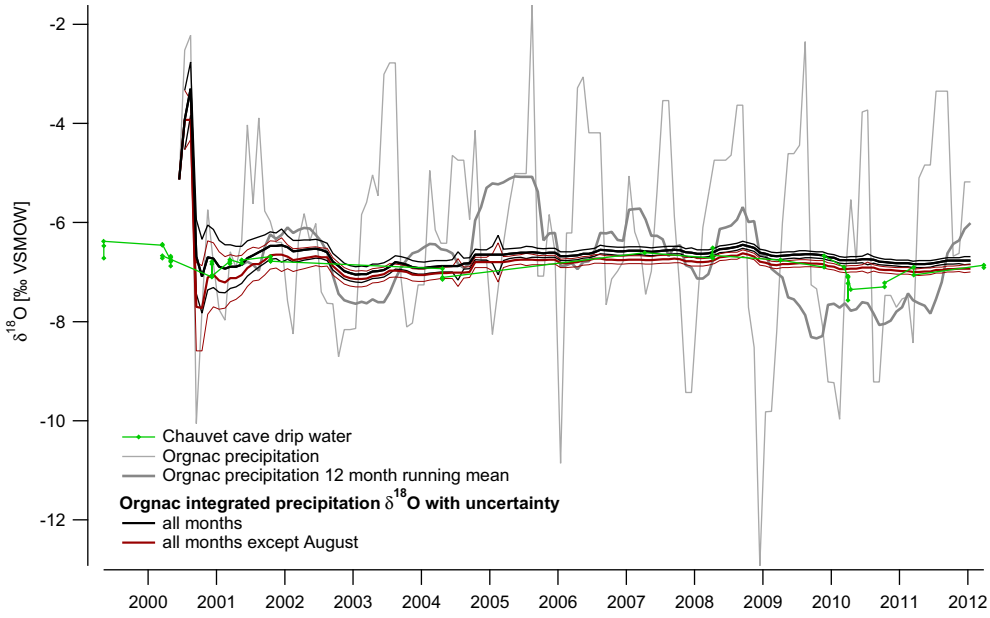

Fig. 11. Precipitation and drip water $\delta^{18}O$ at Chauvet cave. The thin grey line is the Orgnac precipitation $\delta^{18}O$. The green line is the drip water $\delta^{18}O$ from different stations in Chauvet cave. It is compared to (1) a 12 month running mean of precipitation $\delta^{18}O$ weighted by the amount of precipitation (it considers all months of the year; thick grey line); (2) the integrated precipitation $\delta^{18}O$ for all months (black) and for all months except August (brown) with their respective uncertainties. (For interpretation of the references to colour in this figure legend, the reader is referred to the web version of this article.)

Table 7
Stable isotope values and drip characteristics of the dripping water at different monitoring stations in Villars and Chauvet Cave.

Station	$\delta^{18}O$	1σ	δD	1σ	N	L/year	$\Delta\ \delta^{18}O$	Δ drip rate
Villars-Vil#1A	−6.38	0.06	−39.52	0.83	73	375	0.37	2.57
Villars-Vil#1B	−6.39	0.05	−39.62	0.63	82	1419	0.25	8.87
Villars-Vil#10A	−6.17/−6.13	0.22	−37.17	1.72	91	1326	1.35	12.84
Villars-Vil#10B	−6.17	0.07	−37.34	0.90	74	334	0.44	2.5
Chauvet-all	−6.89	0.22	−42.76	1.89	53			

N is the number of samples, σ is the standard deviation, L/year is the mean annual quantity of water from a station, $\Delta\ \delta^{18}O$ is the maximum $\delta^{18}O$ amplitude between min and max $\delta^{18}O$ during the observation period, Δ drip rate is the maximum amplitude between min and max drip rate during the observation period. Mean annual drip water $\delta^{18}O$ have been weighted by the drip rate of each station and gave similar results to the unweight $\delta^{18}O$, only Villars-#10A displays a slight difference which close to the analytical uncertainty, −6.13 being the weighted value.

(Fig. 10, Table 7). Chauvet Cave consists of only one level, and there is not enough data available to have a long continuous series for each sampling station, which is why all the drip water data were averaged. Only Villars station #10A displays significant $\delta^{18}O$ variations of up to 1.2‰ (Fig. 10), which is likely due to its more direct connection with the surface, as suggested by its relatively high drip-rate variability (Genty, 2008). The other stations (#10B, #1A, #1B) have very stable values, which means that they represent a mixing of the rainfall input over several months or years, similar to previous studies (Yonge et al., 1985; Chapman et al., 1992; Williams and Fowler, 2002). The link between the rainfall $\delta^{18}O$ and the cave drip water $\delta^{18}O$ is explored in the following sections.

4.2.2. Discussions

4.2.2.1. Cave water isotopic composition modeling and infiltration residence time. The time during which precipitation is integrated in the rock formation above the cave is crucial for estimating the effective age of drip water. At both sites Villars and Orgnac, the weighted annual mean of precipitation $\delta^{18}O$ (i.e. 12 months averaging) varies from year to year by up to 3‰ (Figs. 10b and 11). When calculating a weighted mean of the months during which the water excess (precipitation minus potential evapotranspiration (PET)) is positive (by using this method we discarded the possibility of infiltration during dry months, which might still be possible for intense rain events), which is between October/November and April/May for this area (Genty, 2008), the year-to-year variability is as high as that for the annual mean (not shown). Since the drip water isotopic composition in both caves is constant, the stalagmites must be fed by water which has a residence time in the soil and in the bedrock above the cave greater than one year. This is also the reason why it is not necessary to weight the drip water by the drip rate when comparing to the rainfall data. One way to determine the residence time of the seepage water is to integrate, month by month, the

weighted rainfall $\delta^{18}O$ since the beginning of measurements and to compare this against the drip water $\delta^{18}O$ values. The number of integrated months required to reach the cave water $\delta^{18}O$ value should provide a reliable estimate of the minimum duration of rainfall mixing. Our hypothesis is that seasonal rainfall $\delta^{18}O$ does not change considerably from one year to the other (i.e. there are no exceptional years that would significantly modify the underground reserve $\delta^{18}O$) and that there is no change in the isotopic signature during infiltration (Lastennet, 1994). Furthermore, we use local data which is sampled directly above the respective caves and not modeled or interpolated from nearby stations. Integrated rainfall $\delta^{18}O_{int}$ is then defined as:

$$\delta^{18}O_{int} = \frac{\Sigma P * \delta^{18}O}{\Sigma P}$$

In order to determine which months contribute to the recharge, we first considered that rainfall feeds the karst water reserve when the water excess is positive, as proposed in former studies (e.g. (Genty and Deflandre, 1998)). Then, depending on the results, the number of months that contribute to the recharge was increased, until the integrated $\delta^{18}O$ reached the cave $\delta^{18}O$ value. If only the months with a positive water excess are considered, when infiltration to the underground should theoretically occur, we obtain integrated rainfall $\delta^{18}O$ values which are much lower than the cave drip water values. The best fit is obtained by integrating all months, or by removing only August, the hottest month (Fig. 10). This implies that the rainfall of the whole year contributes to the recharge, even in summer when the PET is large, producing a low water excess (Fig. 6). A study of soil water $\delta^{18}O$ in the Netherlands also demonstrated that the whole year's precipitation contributes to groundwater recharge, despite a soil-moisture deficit in summer and a precipitation surplus during the winter (Gehrels, 1998). The authors explain this by preferential flow which dominates soil water movement. Certainly, water is lost from the soil to the atmosphere during months with a large PET, but mainly through the vegetation cover and not through direct evaporation from the soil, which would modify the isotopic composition of the remaining soil water. This is true for the studied sites where there is no bare soil but only forest and grass cover. There is generally no fractionation of isotopes when water is taken up by plant roots (Obrist et al., 2004). Furthermore, at these sites we assume that there is minimal seasonal bias introduced by transpiring plants, which could theoretically only take up water consisting of, for example, the growing season precipitation. Such a process would lead to a cave drip water that is composed to a large part of non-growing season precipitation. Apparently this is not the case, since the cave drip water's isotopic composition corresponds to the weighted mean of all months' precipitation. An important consequence of this finding for the interpretation of tree ring cellulose $\delta^{18}O$ is that trees – at least at this site – use mixed water with a certain residence time in the soil, which represents several years' precipitation. Alternatively, the cave drip water $\delta^{18}O$ values could be explained by a mixing of: (1) rain water that infiltrates when the water excess is positive (i.e. between October/November and April/May); and (2) summer precipitation which is enriched by evaporation. Since a part of the summer precipitation is lost to the atmosphere in this process, its contribution to the weighted mean $\delta^{18}O$ would be smaller, but its higher isotopic value would give the same result. It is not possible to quantify the water loss and isotopic enrichment of the remaining soil water, because direct soil water measurements are not available and would be difficult to perform in karstic terrains where the soil layer is thin and irregular. But, whatever the hypothesis concerning the seasons which contribute to the recharge, the only way to explain the great stability of the cave drip water $\delta^{18}O$ is to consider mixing of rainwater spanning several years in a reservoir, and, by doing this, the only way to reach the mean drip water values, is to consider either all months of the year or all months except August (Figs. 10 and 11). Removing more summer months in the calculations leads to too low values.

Fig. 10 shows that the actual $\delta^{18}O$ value of the lower gallery lies between the two curves: the integrated rainfall $\delta^{18}O$ value among the entire period (~14 years) for all months (black thick curve, Fig. 10b) and the integrated rainfall $\delta^{18}O$ for all months except August, the hottest month (brown thick curve). This implies that there is a small deficit of heavier rainfall water due to evaporation during a few days for the entire year. However, given the uncertainties of the measurements, the integration, and the insufficient period of survey (there is still a slight decreasing trend in the integrated rainfall $\delta^{18}O$ curves), we can only conclude that, at Villars, rainfall contributes to underground recharge during the entire year or the entire year minus the month of August. Consequently, it appears that vegetation transpiration does not produce significant seasonal bias in the isotopic signal of the seepage water at this site.

The Chauvet Cave drip water $\delta^{18}O$ time series has much fewer data points, which is why only one time series was constructed using different drip stations. The variability between these locations is relatively low, because the bedrock thickness above them is about the same, although it is still higher than in Villars (Fig. 11). As for the Villars site, the mean drip water value ($-6.89‰ \pm 0.22$) is reached only when considering all months, or all months except August (Fig. 11). Contrary to Villars, the integrated $\delta^{18}O$ value becomes stable very early, after about half a year. Here too, it appears that rainfall during the whole year contributes to the recharge. The slightly lower drip water values of the year 2010 might signify a lower contribution to the warmest days/months, but a more frequent sampling would be necessary to be more affirmative.

The integration of monthly precipitation $\delta^{18}O$ values at Villars shows that the upper gallery's drip water $\delta^{18}O$ value (~$-6.17‰$) is reached after about ~28 months for both tests (integration on all months of the year, or on all months except August), whilst for the lower gallery, 15 m deeper, the $\delta^{18}O$ value (~$-6.39‰$) is reached only after about ~140 months if we consider all months (Fig. 10b) and after ~94 months if we consider all month except August (Fig. 10c). All other tests with less summer water for the recharge contribution lead to too low $\delta^{18}O$ values and shorter time integration (considering or not all months of

the year) lead to too high $\delta^{18}O$ variability. Although infiltration times may be much shorter (i.e. a few weeks in the very well drained karst (10–20 m thick) of Black Chasm Cavern, California (Oster et al., 2012) or a few months in Nerja Cave, south Spain (for 30 m thickness), (Carrasco et al., 2006)), these surprisingly long durations are coherent with previous studies that investigated the seepage water residence time in caves with stable isotopes and tritium. Vertical travel time in Carlsbad Cavern, New Mexico, was found to be of the order of decades for depth up to 250 m (Chapman et al., 1992); it takes 26–36 years for the rain water to reach galleries 10–50 m below the surface in Soreq Cave, Israel (Kaufman et al., 2003); and it takes about 2–4 years to reach galleries at 10–30 m depth in Bunker Cave, Germany (Kluge et al., 2010). Considering the average depth of the galleries, the residence times found in Villars Cave are close to the ones found in Soreq Cave.

4.2.2.2. Insights into the Villars Cave drip water $\delta^{18}O$ and flow rate behavior. More information can be extracted from Villars Cave, where the drip water was studied at two different levels, and at two stations, close each other (1–4 m), at each level. We observe the following (Table 7; Fig. 12):

(1) all four stations display a great stability in the drip water $\delta^{18}O$ values since the beginning of observations;
(2) average drip water $\delta^{18}O$ values are similar for each gallery, weighted or not by the drip rate (because of the stability of the $\delta^{18}O$ and despite the seasonal changes in the drip rates);
(3) there is a small (−0.2‰) but significant (±0.09) difference between the upper (#10A, #10B) and lower (#1A, #1B) galleries drip water $\delta^{18}O$, the lower gallery stations $\delta^{18}O$ being lower (-6.38‰) compared to the upper gallery ones (-6.17‰);
(4) the highest $\delta^{18}O$ variability is observed in the stations from the upper gallery;
(5) there is no link between the mean quantity of water that flowed under the stalactites and the depth of the galleries: stations #10A (upper) and station #1B (lower), display the highest flow rates, four times higher than the nearby stations;
(6) but there is a link between the mean annual drip rate and the variability of the flow: the highest the mean flow rate, the highest the variability, whatever the depth of the gallery;
(7) the drip rate variations show well marked seasonal variability in all the stations; the amplitude of this seasonality is not linked with the depth of the galleries; since the beginning of the observation, dripping never stopped in all these stations;

Indeed, these data confirm the great heterogeneity of the karst aquifer: because of the complexity of the micro-fractures network in the karst above caves, it is very likely that different conduits and fractures with different types of flow rates (i.e. diffuse, preferential), contribute to the reservoir that feed the stalactite drips (White, 1988; Bar-Matthews et al., 1996; Tooth and Fairchild, 2003; Baker et al., 2010; Bradley et al., 2010; Fairchild and Baker, 2012). A good illustration of this is the difference observed in the high resolution drip flow rate measurements between #10A and #10B, only 4 m from each other, and where a significant delay of several weeks in the autumn/winter seasonal flow rate increase was observed coupled with a difference in the flow rate amplitudes (Fig. 13 and Table 1 in (Genty, 2008)). The residence times found in our study are thus likely an average time of different hydrological components, fast (hours to days) and slow (days to months to years) at a specific place in the cave, for this reason we can call them "apparent residence times".

But stable isotope data bring here new light in the understanding of the origin of the drip water feeding stalagmites. First, it appears that there is no link between the hydrological behavior (flow rate quantity, variability) and the mean drip water $\delta^{18}O$ in each gallery, weighting or

Fig. 12. Drip water $\delta^{18}O$ (top) and flow rates (bottom) at four monitoring stations in Villars cave. Note the well marked seasonality in the drip rates, while the oxygen isotope composition stays very stable for #1A, #1B and #10B. The higher variability at station #10A is likely due to a more direct fracture network connection of this stalactite with the outside.

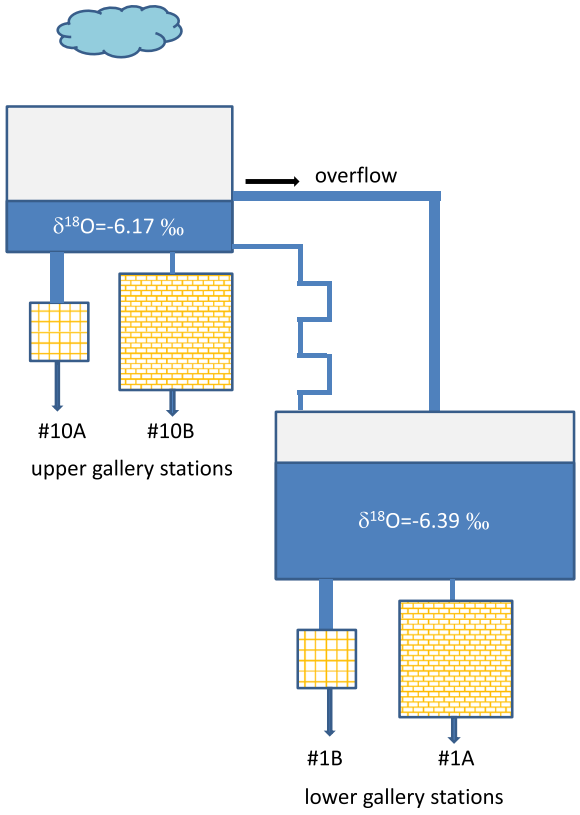

Fig. 13. Conceptual model of the infiltration in the Villars Cave. Rainwater fills a first reservoir, where mixing of precipitation during all the year leads to a mean $\delta^{18}O$ of −6.17‰. This reservoir feeds sub-reservoirs of station #10A and #10B. Differences in capacity and fracture size explain the different drip flow behavior (#10A shows a much higher seasonal amplitude; see Fig. 12 and Table 7) of these two stations which have a similar $\delta^{18}O$. During humid periods (i.e. winter, spring), overflows feed a second larger reservoir, which is also fed by a more regular flow from the first reservoir giving a final value of $\delta^{18}O$ of −6.39‰. This reservoir feeds sub-reservoirs connected to #1A and #1B. Like for the upper level, differences in capacity and fracture size explain the different drip flow behavior (#1B shows a much higher seasonal amplitude).

not these measurement do not change anything in the average values; second, the significant difference between the upper and lower galleries drip water $\delta^{18}O$ raises questions about its cause; third, the fact that the lower galleries have the lowest drip water $\delta^{18}O$ and also have the highest stability leading to longest apparent residence times might be connected to the former observation.

The independence between the drip rate and the $\delta^{18}O$, combined with the perennial dripping (i.e. no drying), confirms the existence of a mixing reservoir above each gallery that has a piston flow functioning: rainfall recharges a water reserve, more or less large, that feed the stalactites/stalagmite system. The existence of such a reservoir is already known and was describes in several other studies (i.e. see references in (White, 1988; Genty and Deflandre, 1998; Ford and Williams, 2007; Baker et al., 2010; Fairchild and Baker, 2012)). Already known also is the heterogeneity of the fractures/conduits that leads to different types of flow (slow/fast; diffuse/preferential etc. see above references). But recent hypotheses combining hydrology and water isotopes during infiltration in karst suggest that variations in the hydrological routing might occur and may explain offsets in drip water $\delta^{18}O$ compared to weighted mean $\delta^{18}O$ of precipitation (Bradley et al., 2010). Overflows or bypass flows could be the cause of lower drip water $\delta^{18}O$ when they are activated by high recharge periods (i.e. winter during which the rainfall $\delta^{18}O$ is lower). This would be a tempting hypothesis in order to explain the lower $\delta^{18}O$ of the lower gallery drips in Villars Cave (Fig. 13): rainfall flows into a first reservoir, with a mean $\delta^{18}O$ of −6.17‰, which feeds the upper gallery stations #10A and #10B; overflows, that are more likely to occur during winter and spring, go into another reservoir through preferential conduits, this reservoir, with a lower mean $\delta^{18}O$ (−6.39‰), feeds the two deepest stations in Villars (#1A and #1B). We suggest that this reservoir is also mainly fed by the upper reservoir with smaller fractures or more diffuse infiltration and that its lower $\delta^{18}O$ value is the result of a mixing of both overflows and regular seepage. Finally, its size, likely larger than the upper reservoir, might explain its longer time residence.

Another hypothesis could explain the $\delta^{18}O$ difference between upper and lower galleries in Villars Cave: because the apparent time residence of the lower gallery drip water is longer, we can suggest that the mean rainfall $\delta^{18}O$ was lower during the past decades and its imprint arrives in the present days in the seepage water. This hypothesis is reinforced by the local air temperature records which show a significant lower air temperatures (by about 2–3 °C) during the winter season before the years 1987 (i.e. Fig. 17 in (Genty, 2008)).

4.2.2.3. Drip water and LMWL. The local meteoric water lines (LMWL) of Villars, Le Mas and Orgnac show close similarities and are characterized, like most rainfall stations, by large seasonal variations (Fig. 5). Due to the large number of measurements, and to the good analytical accuracy, we confirm here a second and important characteristic of cave waters: the gravity centre of the cave isotopic clouds are slightly above the LMWL (Fig. 5). This specific feature was already noted for Villars (Genty, 2008), and is confirmed here by the Chauvet data. A possible explanation for such an offset slightly above the meteoric line would be a contribution of condensed water to drip water (Clark and Fritz, 1999). Studying moonmilk deposits and cave waters in the Caverne de l'Ours (Canada), Lacelle et al. found out that the condensed water on the cave walls that feed the deposits was situated above the local meteoric water line (Lacelle et al., 2004). It is well known that there are condensation zones near cave entrances due to the interaction between outside air and cave air (Ford and Williams, 2007). It has been observed in many caves that condensed water flows along walls, vaults and external surfaces of stalactites and forms drops at the stalactites tips, similar to regular seepage water. Such phenomena can occur in galleries and conduits that are located in the upper part of the karst, close to the surface, where temperature variations are large. More measurements are needed to confirm this hypothesis, and sampling of condensation water in such zones is in progress.

5. CONCLUSIONS

The comparison between 12- and 16-year-long rainfall isotope series of and on-site cave waters in two different regions of south France allows a better understanding of the isotope signal of the drip water which feeds stalagmites. Comparison of these isotopic series with meteorological data and numerical model simulations bring information about the controlling factors that constrain the water $\delta^{18}O$ in these areas. The main results are:

(1) in the two studied caves, Villars (north SW-France, Atlantic climate influence) and Chauvet (SE-France; Atlantic/Mediterranean climate influences), all the stalactite drip stations, from 10 to 50 m depth from the surface, display a remarkable stability in their isotopic composition since the beginning of measurements (i.e. >10 years);
(2) the average $\delta^{18}O$ values of these cave drips do not correspond to the weighted mean annual value of rain water $\delta^{18}O$, neither when considering all the months, nor with the months during which water excess is theoretically positive;
(3) the very stable isotopic signal of cave drip waters can only be explained by considering a mixing of rainwater over several months to several years (up to 32 and to 140 months for the lower galleries of Villars Cave) and an infiltration of rainwater during all months of the year or all months except August. This result is of great importance for the interpretation of speleothem and tree rings isotopic measurements for two main reasons: (a) at least at present, there is no seasonal bias in the $\delta^{18}O$ of cave drip water, which means that fluid inclusions recovered from speleothems should represent the mean annual (or pluri-annual) rainfall water composition unless local evaporation changes its composition; (b) the vegetation above the cave (trees, grass), despite an important water consumption, does not provoke any seasonal bias as it would be the case if they used only spring/summer waters. On the contrary, they use the water from reserves that are already mixed for several months/years. This has important consequences for the interpretation of tree ring cellulose $\delta^{18}O$;
(4) at Villars Cave, the drip water $\delta^{18}O$ of the lower galleries is significantly lower (−0.2‰) compared to the upper galleries; this could be the consequence of overflows that feed lower reservoirs and/or to older rainwater that reach the lower galleries at present days and which were formed during a colder period as it is shown buy the local air temperature records;
(5) the relationship between rainfall $\delta^{18}O$ and surface air temperature shows slopes between 0.14 and 0.18‰/°C at the monthly scale and between 0.47 and 0.57‰/°C at the annual scale; there is a weak correlation between the weighted rainfall $\delta^{18}O$ and the mean air temperature, considering mean air temperature of all days or mean air temperature of rainy days only;
(6) local meteoric water lines (LMWL) have been characterized in three different rainfall stations: Villars and Le Mas (north SW-France) and Orgnac (close to Chauvet Cave; SE-France); they display very similar slopes, close to 7, but show slight differences in the seasonal variability has seen in monthly isotopic graphs: $\delta^{18}O$ variability is much higher in winter than in summer and presents an abrupt isotopic threshold which is observed between August and September. This threshold effect is particularly well marked at the Orgnac station, likely due to its more Mediterranean climate;
(7) comparison between rainfall $\delta^{18}O$ measurements and REMOiso simulations show a systematic overestimation of the $\delta^{18}O$ by the model. This holds both for the annual mean and for the seasonal amplitude at all stations. However, despite the short-duration period where a direct comparison was possible, REMOiso apparently simulates many features of the observed isotope signals. In particular, the model reproduces some interesting patterns of the observed intra-seasonal variability, such as isotopic double peaks, which appear in winter at all stations and which are not related to surface air temperature or precipitation. However, our finding of common intra-seasonal variability needs to be confirmed on longer time scales both for observations and for model simulation. The model's evaluation here suggests that the modeling technique of nudging a regional model within a global model employed here is sufficiently suitable for obtaining reliable rainfall isotopic times series on much longer time scales, which are needed for a reliable proxy interpretation.

ACKNOWLEDGEMENTS

This long study on Villars Cave was possible only with the constant help of the Versaveau family, who have always shown interest in our research. We are very grateful to the family and to the guides of the cave. We also thank M. Maurice Ducros for gathering meteorological data at Orgnac, as well as the Orgnac manager Joël Ughetto, who always encouraged us. We thank J.M. Geneste and his research team for their help and support all along the study of the Chauvet Cave. Finally, we thank our faithful friend and caver Thierry Baritaud for all his precious help. This study was funded by the LSCE/CEA/CNRS laboratory, the CNRS INSU program PALEOMEX-ISOMEX (MISTRAL) and the Rhône-Alpes DRAC.

APPENDIX A. SUPPLEMENTARY DATA

Supplementary data associated with this article can be found, in the online version, at http://dx.doi.org/10.1016/j.gca.2014.01.043.

REFERENCES

Anderson W. T., Bernasconi S. M., McKenzie J. A., Saurer M. and Schweingruber F. (2002) Model evaluation for reconstructing

the oxygen isotopic composition in precipitation from tree ring cellulose over the last century. *Chem. Geol.* **182**, 121–137.

Bakalowicz M. and Jusserand C. (1986) Etude de l'infiltration en milieu karstique par les méthodes géochimiques et isotopiques. Cas de la grotte de Niaux (Ariège, France). *Bull. Centre d'hydrol. Univ. Neuchâtel* **7**, 265–281.

Baker A., Asrat A., Fairchild I. J., Leng M. J., Thomas L., Widmann M., Jex C. N., Dong B. W., van Calsteren P. and Bryant C. (2010) Decadal-scale rainfall variability in Ethiopia recorded in an annually laminated, Holocene-age, stalagmite. *Holocene* **20**, 827–836.

Bar-Matthews M., Ayalon A., Matthews A., Sass E. and Halicz L. (1996) Carbon and oxygen isotope study of the active water–carbonate system in a karstic Mediterranean cave: implications for paleoclimate research in semiarid regions. *Geochim. Cosmochim. Acta* **60**, 337–347.

Bottrell S. H. and Atkinson T. C. (1992) Tracer study of flow and storage in the unsaturated zone of a karstic limestone aquifer. *Tracer Hydrol.*, 207–211.

Bradley C., Baker A., Jex C. N. and Leng M. J. (2010) Hydrological uncertainties in the modelling of cave drip-water delta O-18 and the implications for stalagmite palaeoclimate reconstructions. *Quatern. Sci. Rev.* **29**, 2201–2214.

Caballero E., DeCisneros C. and Reyes E. (1996) A stable isotope study of cave seepage waters. *Appl. Geochem.* **11**, 583–587.

Carrasco F., Andreo B., Linan C. and Mudry J. (2006) Contribution of stable isotopes to the understanding of the unsaturated zone of a carbonate aquifer (Nerja Cave, southern Spain). *C.R. Geosci.* **338**, 1203–1212.

Celle H., Daniel M., Mudry J. and Blavoux B. (2000) Rainwater tracing using environmental isotopes in the western Mediterranean region. Case of the region of Avignon (Southeast France). *C.R. Acad. Sci. Ser., Ii Fascicule a–Sci. Terre Et Des Planetes* **331**, 647–650.

Celle-Jeanton H., Gonfiantini R., Travi Y. and Sol B. (2004) Oxygen-18 variations of rainwater during precipitation: application of the Rayleigh model to selected rainfalls in Southern France. *J. Hydrol.* **289**, 165–177.

Celle-Jeanton H., Travi Y. and Blavoux B. (2001) Isotopic typology of the precipitation in the Western Mediterranean region at three different time scales. *Geophys. Res. Lett.* **28**, 1215–1218.

Chapman J. B., Ingraham N. L. and Hess J. W. (1992) Isotopic investigation of infiltration and unsaturated zone flow processes at Carlsbad Cavern, New Mexico. *J. Hydrol.* **133**, 343–363.

Clark I. D. and Fritz P. (1999) *Environmental Isotopes in Hydrology*. CRC Press, Boca Raton, London, New York.

Cruz F. W., Karmann I., Viana O., Burns S. J., Ferrari J. A., Vuille M., Sial A. N. and Moreira M. Z. (2005) Stable isotope study of cave percolation waters in subtropical Brazil: implications for paleoclimate inferences from speleothems. *Chem. Geol.* **220**, 245–262.

Daeron M., Guo W., Eiler J., Genty D., Blamart D., Boch R., Drysdale R., Maire R., Wainer K. and Zanchetta G. (2011) (13)C(18)O clumping in speleothems: Observations from natural caves and precipitation experiments. *Geochim. Cosmochim. Acta* **75**, 3303–3317.

Daeron M., Guo W., Eiler J., Genty D., Wainer K., Affek H., Vonhof H. and Blamart D. (2008) Absolute speleo-thermometry, using clumped isotope measurements to correct for kinetic isotope fractionations induced by CO(2) degassing. *Geochim. Cosmochim. Acta* **72**. A193-a193.

Dansgaard W. (1964) Stable isotopes in precipitation. *Tellus* **16**, 436–468.

Daux V., Lecuyer C., Adam F., Martineau F. and Vimeux F. (2005) Oxygen isotope composition of human teeth and the record of climate changes in France (Lorraine) during the last 1700 years. *Clim. Change* **70**, 445–464.

De Cisneros C. J., Caballero E., Vera J. A. and Andreo B. (2011) An optimized thermal extraction system for preparation of water from fluid inclusions in speleothems. *Geol. Acta* **9**, 149–158.

Denniston R. F., Gonzalez L. A., Baker R. G., Asmerom Y., Reagan M. K., Edwards R. L. and Alexander E. C. (1999) Speleothem evidence for Holocene fluctuations of the prairie-forest ecotone, north-central USA. *Holocene* **9**, 671–676.

Dublyansky Y. V. and Spotl C. (2009) Hydrogen and oxygen isotopes of water from inclusions in minerals: design of a new crushing system and on-line continuous-flow isotope ratio mass spectrometric analysis. *Rapid Commun. Mass Spectrom.* **23**, 2605–2613.

Fairchild I. and Baker A. (2012) *Speleothem Science*. Wiley-Blackwell.

Fairchild I. J., Tuckwell G. W., Baker A. and Tooth A. F. (2006) Modelling of dripwater hydrology and hydrogeochemistry in a weakly karstified aquifer (Bath, UK): implications for climate change studies. *J. Hydrol.* **321**, 213–231.

Ford D. C. and Williams P. (2007) *Karst Geomorphology and Hydrology*. Wiley.

Friederich H. and Smart P. L. (1981) Dye tracer studies of the unsaturated zone: recharge of the carboniferous limestone aquifer of the Mendip Hills, England. In *Proceedings of the 8th International Congress of Speleology*, Kentucky, pp. 283–286.

Gehrels J. C. a. P. J. E. M. (1998) The mechanism of soil water movement as inferred from 18O stable isotope studies. *Hydrol. Sci.* **43**.

Genty D. (2008) Palaeoclimate research in Villars Cave (Dordogne, SW-France). *Int. J. Speleol.* **37**, 173–191.

Genty D., Baker A., Massault M., Proctor C., Gilmour M., Pons-Branchu E. and Hamelin B. (2001) Dead carbon in stalagmites: carbonate bedrock paleodissolution vs. ageing of soil organic matter. Implication for 13C variation in speleothems. *Geochim. Cosmochim. Acta* **65**, 3443–3457.

Genty D., Blamart D., Ghaleb B., Plagnes V., Causse C., Bakalowicz M., Zouari K., Chkir N., Hellstrom J., Wainer K. and Bourges F. (2006) Timing and dynamics of the last deglaciation from European and North African delta C-13 stalagmite profiles – comparison with Chinese and South Hemisphere stalagmites. *Quatern. Sci. Rev.* **25**, 2118–2142.

Genty D. and Deflandre G. (1998) Drip flow variations under a stalactite of the Père Noël cave (Belgium). Evidence of seasonal variations and air pressure constraints. *J. Hydrol.* **211**, 208–232.

Hoffmann G., Cuntz M.J.J. and Werner M. (2005) How much climate information do water isotopes contain? A systematic comparison between the IAEA/GNIP isotope network and the ECHAM 4 atmospheric general circulation models. In *Isotopes in the Water Cycle: Past, Present and Future of a Developing Science* (eds. P. Aggarwal, J.R. Gat and K. Fröhlich). pp. 303–320. Vienna: International Atomic Energy Agency (IAEA).

Hoffmann G., Jouzel J. and Masson V. (2000) Stable water isotopes in atmospheric general circulation models. *Hydrol. Process.* **14**, 1385–1406.

Hoffmann G., Werner M. and Heimann M. (1998) Water isotope module of the ECHAM atmospheric general circulation model: a study on timescales from days to several years. *J. Geophys. Res.-Atmos.* **103**, 16871–16896.

IAEA (1997) Technical Procedure for cumulative monthly sampling of precipitation for isotopic analyses. Accessible at: www-naweb.iaea.org/NAALIHL/docs/tech_info/Precipitation%20Sampling97.pdf.

IAEA/WMO (2006) Global Network of Isotopes in Precipitation. The GNIP Database. Accessible at: http://www.iaea.org/water.

Jacob D. (2001) A note to the simulation of the annual and inter-annual variability of the water budget over the Baltic Sea drainage basin. *Meteorol. Atmos. Phys.* **77**, 61–73.

Jacob D. and Podzun R. (1997) Sensitivity studies with the regional climate model REMO. *Meteorol. Atmos. Phys.* **63**, 119–129.

Joussaume S., Sadourny R. and Jouzel J. (1984) A general-circulation model of water isotope cycles in the atmosphere. *Nature* **311**, 24–29.

Kaufman A., Bar-Matthews M., Ayalon A. and Carmi I. (2003) The vadose flow above Soreq Cave, Israel: a tritium study of the cave waters. *J. Hydrol.* **273**, 155–163.

Kluge T., Riechelmann D. F. C., Wieser M., Spotl C., Sultenfuss J., Schroder-Ritzrau A., Niggemann S. and Aeschbach-Hertig W. (2010) Dating cave drip water by tritium. *J. Hydrol.* **394**, 396–406.

Kohn M. J. and Welker J. M. (2005) On the temperature correlation of delta O-18 in modem precipitation. *Earth Planet. Sci. Lett.* **231**, 87–96.

Lacelle D., Lauriol B. and Clark I. D. (2004) Seasonal isotopic imprint in moonmilk from Caverne de l'Ours (Quebec, Canada): implications for climatic reconstruction. *Can. J. Earth Sci.* **41**, 1411–1423.

Lastennet R. (1994) *Rôle de la zone non saturée dans le fonctionnement des aquifères karstiques*. Avignon, Avignon, p. 239.

Lecolle P. (1983) Correlation between O-18 and C-13 Isotope Ratios of Land Snails and the Oceanic and Alpine Climates. *C.R. Acad. Sci. Ser., Ii* **297**, 863–866.

Lecolle P. (1985) The oxygen isotope composition of landsnail shells as a climatic indicator – applications to hydrogeology and paleoclimatology. *Chem. Geol.* **58**, 157–181.

Marlin C., Dever L., Vachier P. and Courty M. A. (1993) Chemical and isotopic changes in soil–water during refrosting of an active layer on continuous permafrost (Brogger-Peninsula, Svalbard). *Can. J. Earth Sci.* **30**, 806–813.

Matthews A., Ayalon A. and Bar-Matthews M. (2000) D/H ratios of fluid inclusions of Soreq cave (Israel) speleothems as a guide to the Eastern Mediterranean Meteoric Line. *Chem. Geol.* **166**, 183–191.

McCarroll D. and Loader N. J. (2004) Stable isotopes in tree rings. *Quatern. Sci. Rev.* **23**, 771–801.

McDermott F. (2004) Paleo-climate reconstruction from stable isotope variations in speleothems: a review. *Quatern. Sci. Rev.* **23**, 901–918.

McDermott F., Atkinson T. C., Fairchild I. J., Baldini L. M. and Mattey D. P. (2011) A first evaluation of the spatial gradients in delta(18)O recorded by European Holocene speleothems. *Global Planet. Change* **79**, 275–287.

Obrist D., Yakir D. and Arnone J. A. (2004) Temporal and spatial patterns of soil water following wildfire-induced changes in plant communities in the Great Basin in Nevada, USA. *Plant Soil* **262**, 1–12.

Oster J., Montanez I. and Kelley N. (2012) Response of a modern cave system to large seasonal precipitation variability. *Geochim. Cosmochim. Acta* **91**, 92–108.

Rozanski K., Araguas-Araguas L. and Gonfiantini R. (1993) Isotopic patterns in modern global precipitation, in climate change in continental isotopic records. *Geophys. Monogr.* **78**, 1–36.

Rozanski K. and Dulinski M. (1987) *Deuterium content of European Palaeowaters as inferred from isotopic composition of fluid inclusions trapped in carbonate cave deposits*. IAEA-SM-299/99 IAEA-SM-299/99, 565–578.

Rozanski K., Johnsen S. J., Schotterer U. and Thompson L. G. (1997) Reconstruction of past climates from stable isotope records of palaeo-precipitation preserved in continental archives. *Hydrol. Sci. J.–J. Sci. Hydrol.* **42**, 725–745.

Schmidt G., LeGrande A. and Hoffmann G. (2007) Water isotope expressions of intrinsic and forced variability in a coupled ocean-atmosphere model. *J. Geophys. Res.-Atmos.* **112**.

Sjolte J., Hoffmann G., Johnsen S. J., Vinther B. M., Masson-Delmotte V. and Sturm C. (2011) Modeling the water isotopes in Greenland precipitation 1959–2001 with the meso-scale model REMO-iso. *J. Geophys. Res.-Atmos.* **116**.

Sturm C., Hoffmann G. and Langmann B. (2007) Simulation of the stable water isotopes in precipitation over South America: comparing regional to global circulation models. *J. Clim.* **20**, 3730–3750.

Sturm K., Hoffmann G., Langmann B. and Stichler W. (2005) Simulation of delta O-18 in precipitation by the regional circulation model REMOiso. *Hydrol. Process.* **19**, 3425–3444.

Tooth A. F. and Fairchild I. J. (2003) Soil and karst aquifer hydrological controls on the geochemical evolution of speleothem-forming drip waters, Crag Cave, southwest Ireland. *J. Hydrol.* **273**, 51–68.

Treble P. C., Chappell J., Gagan M. K., McKeegan K. D. and Harrison T. M. (2005) In situ measurement of seasonal delta O-18 variations and analysis of isotopic trends in a modem speleothem from southwest Australia. *Earth Planet. Sci. Lett.* **233**, 17–32.

Treydte K., Frank D., Esper J., Andreu L., Bednarz Z., Berninger F., Boettger T., D'Alessandro C. M., Etien N., Filot M., Grabner M., Guillemin M. T., Gutierrez E., Haupt M., Helle G., Hilasvuori E., Jungner H., Kalela-Brundin M., Krapiec M., Leuenberger M., Loader N. J., Masson-Delmotte V., Pazdur A., Pawelczyk S., Pierre M., Planells O., Pukiene R., Reynolds-Henne C. E., Rinne K. T., Saracino A., Saurer M., Sonninen E., Stievenard M., Switsur V. R., Szczepanek M., Szychowska-Krapiec E., Todaro L., Waterhouse J. S., Weigl M. and Schleser G. H. (2007) Signal strength and climate calibration of a European tree-ring isotope network. *Geophys. Res. Lett.* **34**, L24302.

Uppala S., Kallberg P., Simmons A., Andrae U., Bechtold V., Fiorino M., Gibson J., Haseler J., Hernandez A., Kelly G., Li X., Onogi K., Saarinen S., Sokka N., Allan R., Andersson E., Arpe K., Balmaseda M., Beljaars A., Van De Berg L., Bidlot J., Bormann N., Caires S., Chevallier F., Dethof A., Dragosavac M., Fisher M., Fuentes M., Hagemann S., Holm E., Hoskins B., Isaksen L., Janssen P., Jenne R., McNally A., Mahfouf J., Morcrette J., Rayner N., Saunders R., Simon P., Sterl A., Trenberth K., Untch A., Vasiljevic D., Viterbo P. and Woollen J. (2005) The ERA-40 re-analysis. *Q. J. R. Meteorol. Soc.* **131**, 2961–3012.

van Hardenbroek M., Grocke D. R., Sauer P. E. and Elias S. A. (2012) North American transect of stable hydrogen and oxygen isotopes in water beetles from a museum collection. *J. Paleolimnol.* **48**, 461–470.

van Rampelbergh M., Fleitmann D., Verheyden S., Cheng H., Edwards L., De Geest P. and De Vleeschouwer D. (2013) Mid- to late Holocene Indian Ocean Monsoon variability recorded in four speleothems from Socotra Island, Yemen. *Quatern. Sci. Rev.* **65**, 129–142.

von Grafenstein, Erlenkeuser H., Müller J., Trimborn P. and Alefs J. (1996) A 200 year mid-European air temperature record preserved in lake sediments: an extension of the $\delta^{18}O_p$ – air temperature relation into the past. *Geochim. Cosmochim. Acta* **60**, 4025–4036.

von Storch H., Langenberg H. and Feser F. (2000) A spectral nudging technique for dynamical downscaling purposes. *Mon. Weather Rev.* **128**, 3664–3673.

Vonhof H. B., van Breukelen M. R., Hellstrom J. C., Wester W. C. G. and Kroon D. (2008) Fossil dripwater in stalagmites reveals

Holocene temperature and rainfall variation in Amazonia. *Earth Planet. Sci. Lett.* **275**, 54–60.

Vonhof H. B., van Breukelen M. R., Postma O., Rowe P. J., Atkinson T. C. and Kroon D. (2006) A continuous-flow crushing device for on-line delta H-2 analysis of fluid inclusion water in speleothems. *Rapid Commun. Mass Spectrom.* **20**, 2553–2558.

Wackerbarth A., Langebroek P. M., Werner M., Lohmann G., Riechelmann S., Borsato A. and Mangini A. (2012) Simulated oxygen isotopes in cave drip water and speleothem calcite in European caves. *Clim. Past* **8**, 1781–1799.

Wainer K., Genty D., Blamart D., Daeron M., Bar-Matthews M., Vonhof H., Dublyansky Y., Pons-Branchu E., Thomas L., van Calsteren P., Quinif Y. and Caillon N. (2011) Speleothem record of the last 180 ka in Villars cave (SW France): investigation of a large delta(18)O shift between MIS6 and MIS5. *Quatern. Sci. Rev.* **30**, 130–146.

Wang Y. J., Cheng H., Edwards R. L., An Z. S., Wu J. Y., Shen C. C. and Dorale J. A. (2001) A high-resolution absolute-dated late Pleistocene Monsoon Record from Hulu Cave, China. *Science* **294**, 2345–2348.

White B. (1988) *Geomorphology and Hydrology of Karst Terrains*. Oxford University Press, New York, Oxford.

Williams P. W. and Fowler A. (2002) Between oxygen isotopes in rainfall, cave percolation waters and speleothem calcite at Waitomo, New Zealand. *J. Hydrol. (NZ)* **41**, 53–70.

Yonge C. J., Ford D. C., Gray J. and Schwarcz H. P. (1985) Stable isotope studies of cave seepage water. *Chem. Geol.* **58**, 97–105.

Zhang R., Schwarcz H. P., Ford D. C., Serefiddin F. and Beddows P. (2008) An absolute paleotemperature record from 10 to 6 Ka inferred from fluid inclusion D/H ratios of a stalagmite from Vancouver Island, British Columbia, Canada. *Geochim. Cosmochim. Acta* **72**, 1014–1026.

Associate editor: F. McDermott